Title: Thermosensitivity of translation underlies the mammalian nocturnal-diurnal switch

Authors: Andrew D. Beale[1], Nina M. Rzechorzek[1], Andrei Mihut[1], Aiwei Zeng[1], Nicola J. Smyllie[1], Violetta Pilorz[2], Rose Richardson[3], Mads F Bertlesen[4], Nathan R. James[1], Shaline V. Fazal[5], Zanna Voysey[5], Jerry Pelletier[6], Priya Crosby[7], Sew Y Peak-Chew[1], Madeline A. Lancaster[1], Roelof A. Hut[8], John S. O'Neill[1*]

Affiliations:

[1]MRC Laboratory of Molecular Biology; Francis Crick Avenue, Cambridge, CB2 0QH, UK

[2]Institute of Neurobiology, Center of Brain, Behavior & Metabolism, University of Lübeck; Marie Curie Street, 23562, Lübeck, Germany

[3]Centre for Biological Timing, Faculty of Biology Medicine and Health, University of Manchester; Manchester, United Kingdom

[4]Copenhagen Zoo; Frederiksberg, Denmark

[5]Department of Clinical Neurosciences, John Van Geest Centre for Brain Repair, University of Cambridge; Cambridge, CB2 0PY, UK

[6]Department of Biochemistry, McGill University; Montreal, QC, H3G 1Y6, Canada.

[7] Department of Chemistry and Biochemistry, University of California, Santa Cruz; 1156 High Street, Santa Cruz, CA 95064, USA

[8]Groningen Institute for Evolutionary Life Sciences, University of Groningen; 9712 CP Groningen, the Netherlands

*Corresponding author. Email: oneillj@mrc-lmb.cam.ac.uk

Abstract: Early mammals were nocturnal until the Cretaceous-Paleogene extinction facilitated their rapid expansion into daytime niches. Diurnality subsequently evolved multiple times, independently, but the mechanisms facilitating this switch are unknown. We found that physiological daily temperature shifts oppositely affect circadian clock rhythms in nocturnal versus diurnal mammals. This occurs through a cell-intrinsic signal inverter, mediated by global differences in protein phosphorylation, and effected at the level of bulk protein synthesis rates, with diurnal translation rate being less thermosensitive than nocturnal. Perturbations that reduce translational initiation or mTOR activity are sufficient to trigger the nocturnal-to-diurnal switch at the cellular, tissue, and organismal scale. Our results suggest a convergent selection pressure to attain diurnality by reducing the effect of temperature-dependent changes in protein synthesis on circadian clocks.

40 **One sentence summary:** Recalibrating the thermosensitivity of protein synthesis drives daytime-selective activity in mammals.

Main text: Early mammals were nocturnal (night active) until the extinction of the diurnal (day active) dinosaurs facilitated a rapid expansion into daytime niches (*1–3*). Diurnality subsequently arose multiple times, independently, from diverse and distant nocturnal lineages (*1*, *3*). No mechanistic basis for the switch between nocturnality and diurnality is known, though evidently some change in the relationship between internal circadian clocks and external daily rhythms is required (*4*, *5*).

Despite the 76 million years that separate nocturnal mice and diurnal humans from their common ancestor (*6*), the same cell-autonomous circadian clock mechanism operates in both mouse and human cells (*7*). Daily rhythms of gene expression, proteome renewal, and myriad cellular functions depend on cell-intrinsic ~24h oscillations in the production of PERIOD (PER) proteins (*7*, *8*); where the changing activity of PER over time effectively determines the biological time-of-day (*9*). Similarly, the hypothalamic suprachiasmatic nucleus (SCN) functions very similarly in diurnal and nocturnal mammals, receiving light input directly from the eyes to generate an internal representation of solar time (*5*, *10–19*). However, unlike the SCN, PER oscillations in peripheral cells and tissues are oppositely organised between diurnal and nocturnal mammals (*18*, *20*, *21*), and instead vary with daily systemic signals that habitually coincide with the transition from resting, fasting and lower body temperature to activity, feeding and higher body temperature (*22*), rather than external solar time. Thus, excepting the SCN, the major behavioural and physiological daily rhythms in mammals are set to opposite times of day between nocturnal and diurnal mammals (Fig. 1A), suggesting a switch downstream of the SCN (*4*). How diurnal mammals integrate the same environmental cues to achieve an inversion of organismal and cellular physiology compared with nocturnal mammals is an open question, but is critical for understanding mechanisms of internal synchrony that are pivotal for long-term health (*23–26*).

At the cellular level, acute stimulation of PER and/or global protein synthesis elicits similar shifts in the timing (or phase) of subsequent PER oscillations in both mouse and human cells (*9*, *27*, *28*). Physiologically, behavioural patterns of feed/fast, rest/activity, light/dark and stress exposure are major timing cues that act *via* specific systemic signals to synchronise and amplify daily PER oscillations throughout the body (*29–34*), a process known as circadian entrainment (*35*, *36*). However, hormonal entrainment, for example by glucocorticoids (*30*, *31*) and insulin signalling (*22*, *29*, *37*, *38*), occurs very similarly in human and mouse (*29*, *39*). Daily rhythms in body temperature can also synchronise cellular clocks throughout the body and brain, being associated with locomotor/feeding thermogenesis during wakeful activity and increased cooling via peripheral vasodilation during sleep/rest (*40–47*). Whether temperature-mediated timing cues act similarly on cells from diurnal and nocturnal mammals has not previously been tested, however.

Circadian synchronisation by temperature is typically weaker than hormonal stimulation, with heat shock pathway (*45*, *46*), cold shock proteins (*48*, *49*), cdc-like kinases (*50*) and upstream open reading frames (uORFs) in PER mRNA (*51*) having each, separately, been proposed to communicate temperature change to the cellular clock via a range of

transcriptional and post-transcriptional mechanisms (*52–54*). Because these pathways are evolutionarily conserved, circadian responses to temperature change are assumed to operate analogously in mouse and humans. Mouse and human biology can differ markedly, however. Beyond obvious developmental differences (*55*), mouse and human cells can exhibit profoundly different biochemical reaction rates (*56*, *57*).

Here, we show that the sensitivity of bulk protein synthesis to temperature change represents another fundamental difference between nocturnal mice and diurnal humans, with profound physiological consequences that include the nocturnal-diurnal switch. We recapitulate temporal niche selection *in vitro* and reveal its cellular and molecular bases. We identify cell-autonomous differences between nocturnal and diurnal mammals in the response to temperature by specific (PER2 protein synthesis) and general (global phosphorylation and translation rate) mechanisms. Finally, we test the functional consequences of modifying protein synthesis rates on temporal niche *in vivo*, and pinpoint mTOR activity as a nexus of signalling that integrates bioenergetic and temperature cues into the cellular clock.

Results

Nocturnal and diurnal mammalian cellular clocks are differentially affected by daily temperature cycles

Daily temperature cycles can synchronise circadian clocks in cultured mammalian cells and modulate the timing of clock protein activity *in vivo* (*43*, *45*, *46*, *58*). Most systemic timing cues elicit very similar effects on the circadian clocks of mouse and human cells ((*29*, *39*); fig. S1, A and B). We were therefore surprised to find that, using a conventional clock reporter (*Bmal1:luciferase*, *Bmal1:luc*), primary fibroblasts from multiple mice and humans consistently entrained oppositely to gradual 12h:12h 37°C:32°C temperature cycles that mimic daily body temperature rhythms (Fig. 1B, fig. S1C, (*42*, *43*, *46*, *59*)). This is evident from bioluminescence waveforms that rapidly become antiphasic to each other during the temperature cycle, and subsequently persist at constant temperature. Since the clock mechanism, and heat/cold shock pathways, operate similarly in mouse and human cells, this observation is incompatible with previous models of circadian entrainment by temperature (*45*, *46*, *48–51*) and suggests a fundamental difference in the way temperature affects cells from the two species.

Considering this differential synchronisation by temperature to be reminiscent of the opposite temporal niches habitually occupied by mice and humans, we sought to test the generality of our findings using primary fibroblasts from a range of diurnal and nocturnal mammals. In natural environments, humans, marmosets (*60*), sheep (*61*) and striped mice (*62*) occupy diurnal niches whereas rats, mice and lemurs (*63*, *64*) are typically nocturnal. We found that, after temperature cycles, nocturnal representatives consistently entrained oppositely to cells from diurnal species (Fig. 1, C and D). This difference did not associate with body size (Fig. 1D).

To validate our findings, and facilitate deeper mechanistic investigation, we repeated these experiments using an alternative reporter, PER2-LUCIFERASE (PER2-LUC aka PER2::LUC). PER2-LUC is a well-established, reliable reporter of the molecular clock in mammalian cells and tissues (*65*, *66*), since resultant bioluminescence correlates directly with the nascent production of endogenous PER protein (*67*). We compared fibroblasts from PER2-LUC mice (*65*) with human PER2-LUC knock-in cells generated using CRISPR-Cas9 (fig. S2). Again, we found mouse and human cells quickly developed oppositely phased rhythms under a 5°C daily temperature cycle that were maintained under constant conditions (Fig. 1E, fig. S1, D and E).

To confirm our findings were not attributable to any thermal stress response we repeated these experiments with a smaller, 1.5°C, temperature cycle. Again, we observed that human PER2-LUC showed an inverted phase relative to mouse PER2-LUC rhythms (Fig 1, F and G), with the only difference being that entrainment occurred more slowly than under 5°C cycles, with altered phases relative to the temperature cycle (Fig. 1G). This is consistent with theory, i.e., the rate and phase of entrainment varies with the strength of stimulus (Roenneberg et al., 2003). From these observations, we infer that some cell-intrinsic signal inverter must allow the circadian clock in diurnal mammalian cells to respond oppositely to daily temperature cycles

compared with nocturnal cells. This potentially indicates a cellular basis for understanding the diurnal-nocturnal switch.

155

Diurnal cellular clocks are buffered against temperature change by translational control

During entrainment *in vivo*, the phase of cellular clocks is adjusted during each day by systemic signals in a fashion that varies with the magnitude of each stimulus and the
160 relative biological times (circadian phase) at which they are received (*68*, *69*). Having found that daily temperature cycles, in the absence of other synchronising cues, elicited opposite effects on diurnal vs nocturnal cellular clocks, we sought to tease apart the signal inverter mechanism. We first asked whether cellular clocks responded to the temperature increase or decrease, or both, and whether responses differed
165 between mouse and human cells in a way that might account for their differential synchronisation by temperature cycles. As such, mouse and human PER2-LUC cells were subjected to a single temperature increase or decrease at different circadian phases (fig. S3, A-C). From the phase response curves (fig. S3D), it was evident the circadian clock was differentially sensitive to single temperature steps between mouse
170 and human cells. Whilst the qualitative response to temperature change was similar, over most of the circadian cycle, human cells showed greater advances for temperature increase whereas mouse cells showed greater delays for temperature decrease. Under a daily temperature cycle, this would be expected to result in highest PER2 production around the cold-to-warm transition for human cells and opposite for
175 mouse cells, consistent with our observations (Fig.1E).

Acute changes in PER protein production shift the phase of cellular clocks *in vitro* and *in vivo* (*9*, *27*, *29*). We therefore asked whether differential sensitivity of mammalian cellular clocks to temperature change was reflected at the level of PER synthesis. We
180 drew on understanding of firefly luciferase enzyme kinetics (*67*) to deconvolve the acute response to a rapid 5°C temperature increase (Fig. 2A) into two components. First, a baseline increase due to increased catalytic turnover of luciferase, which was not different between mouse and human cells (Fig. 2B); second, the total induction of nascent PER2 protein synthesis, which occurred more rapidly and produced more
185 nascent PER2 in mouse than human cells (Fig. 2C). We considered whether these differences in the acute effect of temperature on PER production might be sufficient to explain differential synchronisation of cells by temperature cycles (Fig. 1, and fig. S1D). Certainly, while antiphasic oscillations were observed in the steady-state and nascent protein levels of PER2 (fig. S3E), only nascent synthesis of PER2 was
190 temperature-sensitive (fig. S3F), and more so in mouse than human cells. Over several cycles then, in principle, species differences in the thermal sensitivity of PER protein production could function cumulatively to invert cellular clock timing. We therefore asked by what mechanisms temperature-dependent translation of PER2 might differ between species. We considered this must either occur by mechanisms
195 that selectively regulate PER or by more general mechanisms that include changes in PER activity.

In terms of selective mechanisms, compared with the clear mouse/human difference in PER2 translation and consistent with previous reports, we found no evidence for
200 equivalent differences in the acute transcriptional response of *Per2* to temperature

change (fig. S4, A and B, (*51*)). This suggests signal inversion occurs post-transcriptionally. As such, we note *Per2* mRNA contains a temperature-responsive upstream open reading frame (uORF) that modulates translation of the PER2 protein (*51*, *70*). The *Per2* uORF is highly conserved among nocturnal and diurnal mammals however (fig. S4C and (*51*), and so not an attractive candidate for species-differences in thermal sensitivity of PER2 production. In contrast, mouse or human PER2-LUC ORF expressed constitutively in mouse or human cells recapitulated the acute response of endogenous PER2-LUC to temperature change (Fig. 2, D and E, fig. S5, A and B), suggesting differential thermal sensitivity of PER2 translation is largely intrinsic to the coding region without requiring 5'- or 3'-UTR regulation. Rare codon usage and RNA secondary structure are common mechanisms of translational regulation that affect the synthesis of many proteins (*71*–*75*), including those with circadian function such as PER2 (*76*, *77*). Consistent with this we found that, compared with wild type, codon-optimised hPER2 (hPER2-CO, fig. S5C) with less predicted mRNA structure (fig. S5D) showed minimal sensitivity to temperature change (Fig. 2, D and E). On the other hand, we identified only modest differences in codon usage and predicted mRNA structure between mouse and human PER2 (fig. S5, C and D), with mouse PER2 slightly more structured than human. Furthermore, PER1 in both species was highly similar (fig. S5, E and F). Thus, it became important to distinguish whether PER2 itself was essential for, or else simply associated with, the signal inverter in diurnal cells.

Therefore, to directly test the contribution of PER2 to circadian synchronisation by temperature cycles, we used CRISPR-edited cells where endogenous HALO-tagged PER2 could be acutely depleted using HALO-PROTAC3 (Fig. 2F, and fig. S6). Critically, when PER2 was acutely depleted, we found significant but only modest differences in the effect of daily temperature cycles on the diurnal cellular clock (Fig. 2G), consistent with previous reports (*51*). Therefore, whilst species-specific differences in PER2 translation may contribute to differential effects of temperature, considered alone, they cannot be the basis for cellular signal inversion. From these data, we do not discount differences in the individual contributions of many other proteins, such as PER1. However, the alternative hypothesis is that global and general diurnal/nocturnal differences in the temperature-dependence of the translational machinery underlie the PER2 translational differences observed hitherto. This alternate hypothesis is informed by recent developmental studies, showing marked differences in global biochemical reactions between species, with humans exhibiting generally slower rates and more stable proteins than mice (*56*, *57*, *78*). We therefore asked whether more general differences in the translational response to temperature change might underpin our observations.

Using constitutively expressed luciferase as a reporter for bulk 5'-cap-dependent translation, we found that mouse cells were much more sensitive to temperature increase and decrease than human cells (Fig. 2, H and I). Mouse cell luciferase production increased with a 5°C temperature increase, and *vice versa*, whereas human cells showed no change for temperature drop and decreased translation for temperature increase. Using 3 independent biological replicates per species, we validated these findings by quantifying nascent polypeptide production with puromycin-labelling (Fig. 2, J-L, and fig. S7A). Again, we found that, unlike in mouse

cells, protein synthesis in human cells was more effectively buffered against physiological temperature change.

The differential effect of temperature on translation rate was also observed over longer timescales: after 1 week at constant 32°C or 37°C, mouse cell protein synthesis was clearly temperature-dependent, faster at the higher temperature, whereas human cells showed no significant difference between the two (Fig. 2M and fig. S7A). Translation in nocturnal rat cells likewise showed differential long-term temperature sensitivity compared with cells from the similarly sized but diurnal grass mouse (Fig. 2M, fig. S7B).

Circadian clocks exhibit the remarkable feature of temperature compensation, where, unlike most biological processes, under constant conditions the ~24h period of oscillation is only modestly affected by a change in ambient temperature (Q_{10} of 0.8-1.2) (*79*, *80*). However, consistent with their increased translational sensitivity to temperature, the cellular clocks of nocturnal mammals show an increased temperature dependence relative to diurnal mammals. Mouse and rat cellular clocks ran ~2h faster at 37°C than 32°C, whereas human and striped mouse cells showed a tendency towards slower clocks at the higher temperature (Fig 2, N and O, and fig. S8, A and B). This provides an additional insight into cellular signal inversion that is complementary to the acute differences in thermosensitivity described above (Fig. S3D): during daily temperature cycles nocturnal cellular clocks accelerate at the higher temperature, whereas diurnal ones tend to slow down.

Circadian clocks drive, and are driven/synchronised, by daily cycles of protein synthesis (*28*, *81–83*). This suggests a simple explanation for cell-intrinsic circadian signal inversion in diurnal mammals. During the transition from nocturnal to diurnal activity, evolution selected for reduced thermal sensitivity of the protein synthesis machinery. In cultured cells, this renders diurnal cellular clocks less thermosensitive, resulting in different phase shifts relative to the temperature change when compared with nocturnal (Fig. 1, fig. S3). Where temperature is the only timing cue, this manifests as a circadian signal inverter when appraised over several days.

In vivo hormonal timing cues, such as daily insulin/iGF-1 signalling linked with feed/fast cycles, act *via* the translational machinery to synchronise cellular clocks throughout the body (*29*). At the organismal scale then, evolutionary adaptions in the thermosensitivity of protein synthesis would be expected to progressively modulate the integration of endocrine timing cues that synchronise cellular clocks throughout body and brain. Being cell-intrinsic, this would inevitably include those neuroanatomical centres that regulate the timing of locomotor and feeding activity to gradually shift the daily organisation of behaviour. Reduced translational sensitivity to temperature could arise through multiple mechanisms, acting at many genetic loci across generations. Conceivably, diurnality it also could be triggered by environmental challenge through epigenetic mechanisms within a generation. Therefore, we next considered the mechanisms that might effect a change in thermosensitivity of the translational machinery, that we hypothesise ultimately underlies the diurnal-nocturnal switch.

Global differences in cellular phosphorylation rates between mouse and human cells involve mTORC1 and contribute to species differences in the thermosensitivity of protein synthesis

300 A key element of protein synthesis control is the phosphorylation of proteins comprising the translational apparatus (*84*), including members of the cap-binding complex eIF4F, 43S preinitiation complex, and the elongation factor eEF2. To gain insight into differential responses to temperature, we performed quantitative (phospho)proteomics on biological replicates of primary mouse and human fibroblasts
305 which had been subjected to high or low temperature either acutely or long term (Fig. 3A, and fig. S9A). We reasoned that thermosensitive phosphosites must impart directionality to temperature signals, and that this must include those that collectively control translation rate. Having already established acute mouse vs human differences in thermosensitivity, we initially focused our analysis on phosphosites where
310 phosphorylation changed proportionally (fold change increases with temperature increase) or in inverse proportion (fold change decreases with temperature increase) with temperature change (Fig. 3B and table S1). After filtering for phosphopeptides detected in all conditions, we detected 6904 and 5690 phosphopeptides in mice and humans respectively. Of these, relative to temperature change, in mice 80 changed
315 proportionally and 768 changed inversely, whereas in humans 463 changed proportionally and 215 changed inversely. Conversely, protein abundances were much less sensitive to acute temperature change in both species (fig. S9, B to H and table S1).

320 We first noted little overlap between mouse and human cells in the specific identity of temperature-dependent phosphosites and of the proteins to which they belong, supporting the idea of global and collective, rather than highly specific, differences in thermosensitivity. This is reinforced by the clear majority of temperature-dependent sites being oppositely regulated between mouse and human cells (Fig. 3B). In mouse,
325 motif analysis for amino acids surrounding the phosphoacceptor (S/T/Y) showed acidic residues were highly enriched for proportional phosphorylations whereas basic residues were highly enriched for inversely proportional phosphorylations (Fig. 3C). In humans these trends were reversed, although overall enrichment in both directions was much reduced relative to mouse, reflecting a generally reduced thermosensitivity
330 of human post-translational regulation, as with translation rate. However, a significant enrichment of basic amino acids in the -2/3 positions upstream of the phosphoacceptor was quite evident in human cells for proportional phosphosites, the mirror of mouse cells. This opposite relationship was also seen in the pattern of residues depleted from phosphoacceptor-adjacent motifs (fig. S10).

335

One explanation for these patterns in amino acid enrichment and depletion is in the collective function of the kinases and/or phosphatases that target these motifs. The enrichment of basic residues around proportional phosphosites in mice, and reversed in humans, is consistent with motifs recognised by basophilic kinases of the AGC and
340 CAMK families, and the cdc-like kinases (CLK) (*85*, *86*). Intriguingly, CLK has been previously suggested to play a role in body temperature sensing (*50*). However, inhibition of CLK1/4 using TG003 (*87*) did not alter the phases of human nor mouse cells under daily temperature cycles (fig. S11). Indeed, a panel of small molecule inhibitors of kinases previously implicated in circadian temperature sensing revealed

345 only modest effects on entrained phase under daily temperature cycles. The largest species-dependent difference was observed for ERK1/2 inhibition (fig. S11, E and F), though this was insufficient to invert phase in either case. It is therefore plausible that global differences in acutely thermosensitive protein phosphorylation primarily arise by differential phosphatase activity.

350

The abundance of HSP70, HSP90, or CIRBP, and their regulation by phosphorylation, changed similarly between mouse and human upon temperature shifts or long-term temperature adaption (fig. S9, C-H), consistent with their cellular response to temperature being conserved between species (*88–90*). Moreover, neither inhibition
355 nor activation of heat shock pathway had any significant differential effect on entrained phase in either human or mouse cells (fig. S11, G and H). Our data are therefore inconsistent with a role for HSF1 signalling (*45*, *46*) or the RNA binding proteins CIRBP and RBM3 (*48*, *49*) in the cell-intrinsic circadian signal inverter.

360 In the alternate hypothesis, signal inversion arises through general and global differences in cellular (de)phosphorylation rates between mouse and human cells. Accordingly, after 1 hour at increased temperature, median phosphorylation significantly increased in human cells but decreased in mouse cells, and vice versa (Fig. 3D top). Moreover, this acute change in phosphoproteome composition was
365 much larger than after 7 days at the new temperature (fig. 3D bottom, fig. S9E), reflecting homeostatic mechanisms of ambient thermo-adaption. This suggests a rapid, and widespread phosphorylation-mediated signalling response to temperature change. Because the motif analysis (fig. 3C) did not highlight the consensus sequence of any single cellular kinase, we infer this occurs through broader differences in the
370 relative thermosensitivity of multiple different kinases and phosphatases. This is consistent with, and very likely underlies, diurnal/nocturnal differences in translational thermosensitivity (Fig. 2).

In light of mouse versus human differences in apparent thermosensitivity of translation
375 rate and basophilic-directed phosphorylation, we investigated mechanistic links between the two. AGC and CAMK are two major basophilic kinase families that include regulators and effectors of mTOR complex 1 (mTORC1)—a master regulator of translational initiation whose activity reflects the integration many different metabolic and extracellular signals (*91–93*). mTORC1 activity shows circadian rhythms in
380 cultured cells, that are amplified by daily feeding rhythms across multiple tissues *in vivo*, to modulate daily rhythms in PER production and ribosome biogenesis, for example (*29*, *94–96*). As such, differential regulation of mTORC1 is a plausible mechanism by which thermal signals to the translational machinery could be inverted. We therefore investigated phosphorylation-mediated regulation of mTORC1 activity
385 by temperature, longitudinally in mouse and human cells. For this, we designed split-luciferase biosensors of kinase activity, which luminesce upon phosphorylation of a target S/T on a sensor domain (Fig. 3E). These were then stably expressed in mouse and human cells under applied temperature cycles. As a control we measured bioluminescence from an activity sensor for acidophilic-directed phosphorylation by
390 casein kinase 1 (CK1, fig. S12, B and C) (*97*). Under daily temperature cycles, CK1 activity was very similar in mouse and human cells (Fig. 3F), showing increased bioluminescence/phosphorylation in the cold portion of the cycle. Unlike CK1,

mTORC1 activity, reported by a novel sensor based on p70S6K1 T412 (fig. S12), was oppositely temperature-dependent in mouse and human cells (Fig. 3G). Consistent with mTORC1-mediated control of protein synthesis rates, oscillations in constitutive LUC expression, a proxy for bulk 5'-cap-directed protein synthesis, from parallel cultures were also inverted between mouse and human cells under identical conditions.

Together, these results suggest the hypothesis that temperature change differentially affects mTORC1 activity which modulates circadian phase *via* a combination of specific (PER synthesis) and more general mechanisms (basophilic kinase activity, bulk translation) which are less thermosensitive in human than mouse cells (Fig. 4A).

Perturbation of translational initiation selectively renders nocturnal cells more diurnal

This hypothesis makes a simple prediction: reducing the basal protein synthesis rate should selectively reduce the capacity of nocturnal cellular clocks to respond appropriately, whereas diurnal cells should be less affected.

To test this, we first sought to reduce the relative magnitude of temperature-dependent differences in translation by reducing the basal protein synthesis rate, thereby attenuating its capacity for thermal variation. Growth factor signalling acts *via* mTORC1 to control protein synthesis rates (*91*, *93*), and can be manipulated in cell culture by changing serum concentration. Under reduced serum concentrations, mouse cellular rhythms were delayed by up to 6h under daily temperature cycles, compared with high serum control conditions, whereas human cells were not (Fig. 4, B and C). Selective mTOR inhibition with INK128 or Torin1 phenocopied this result, as mouse cells showed significant phase delays under daily temperature cycles, but human cells were unaffected (Fig. 4, D and E, fig. S13). Similar treatment of fibroblasts from another nocturnal mammal (rat) and diurnal mammal (striped mouse) gave comparable results (Fig. 4, D and E). In all cases, when mTOR activity was reduced, cells from nocturnal mammals behaved more diurnally under temperature cycles, with PER2-LUC peaks selectively shifting towards the early warm portion of the temperature cycle (Fig. 4, D and E). In other words, nocturnal cells became more similar to diurnal cells under conditions of reduced mTOR activity, whereas the contrary was not true for diurnal cells.

To validate this, we perturbed protein synthesis rates directly, independently of mTOR or temperature change, through pharmacological attenuation of 5'-cap-dependent translational initiation. When treated at the same circadian phase, inhibitors of eIF4A (rocaglamide A, RocA, and hippuristanol) showed very clear and significant differences in the magnitude and direction of circadian phase shifts between mouse and human cells (Fig. 4, G and H). Again, the cellular clock in mouse cells was much more sensitive than in human cells, consistent with our model.

The function of mTOR as a cellular signalling nexus for translational regulation is conserved across eukaryotes, essential in mammals, and so an attractive candidate for mediating the diurnal/nocturnal switch. If so, excepting only the SCN, mTOR inhibition should make circadian clocks in tissues throughout the body and brain behave more diurnally under daily temperature cycles, both *ex vivo* and *in vivo*.

Modifying protein synthesis rates in vivo permits niche switching

To test this, we subjected tissue explants from adult PER2-LUC mice to daily temperature cycles ± mTOR inhibition (Fig. 5A). As expected (*45*, *98*), high amplitude PER2-LUC oscillations were observed in neuroendocrine (pituitary) and non-neuronal (lung, adrenal) tissues, with PER2 consistently peaking around the warm-to-cold transition (Fig. 5, B and C), as in mouse fibroblasts (Fig. 1E). Reduction of mTOR activity by INK128 significantly changed this phase relationship, shifting the PER2-LUC peak by 8-12h around the cold-to-warm transition (Fig. 5C), the same peak time as in human cells (Fig. 1E).

The hypothalamic SCN of nocturnal mammals are remarkable for PER rhythms that are essentially opposite to almost all other tissues, in the same phase as SCN of diurnal mammals (Fig. 1A). This is consistent with the SCN's conserved function in all mammals as a dedicated locus for encoding and communicating anticipated photoperiod. Interneuronal coupling renders SCN PER rhythms more robust than other tissues, and much more sensitive to photic cues than to systemic signals such as temperature (*29*, *45*, *99*). Adult SCN are sensitive to temperature, however, and explants stably entrain to the same daily temperature cycles employed throughout this study (*99–101*). We found that after 7 daily temperature cycles, SCN entrained with a phase that was much later than other tissues, with PER2 peaking late in the cold phase (Fig. 5, C and E), and most reminiscent of the physiological relationship between circadian timing between SCN and other mouse tissues *in vivo*. Remarkably, the phase of SCN rhythms after daily temperature cycles was insensitive to mTOR inhibition (Fig. 5, F and G) - similar to all diurnal cells tested but no other nocturnal cells or tissues. Thus, the circadian clock in SCN of nocturnal mice behaves diurnally with respect to temperature, presumably through a functional insensitivity to mTOR inhibition that renders the protein synthesis machinery less sensitive to temperature change. In other words, mouse brain temperature rhythms are expected to reinforce, rather than interfere with, the SCN's habitual relationship with the light:dark cycle *in vivo*. This is consistent with the SCN's robustness against abrupt changes in translation rate, which is conferred by network coupling (*82*, *102*). Thus, our findings support a model whereby all mammalian SCN maintain a faithful mTOR-insensitive representation of daytime, whereas, beyond the SCN, the daily timing of behaviour and physiology is determined by the interaction between cell-autonomous timekeeping and daily endocrine cues that stimulate daily rhythms in global and specific (PER) protein synthesis *via* mTOR. These are much more thermosensitive in nocturnal than diurnal mammals, and so over consecutive days, daily differences in feedback from locomotor and feeding thermogenesis progressively leads to cells, tissues and animals that occupy opposing temporal niches.

Supporting this, under more natural low net calorie conditions, mouse behaviour and physiology becomes more diurnal than when fed *ad libitum*, whilst SCN rhythms are unaffected (*103–105*). This can be replicated experimentally, using the Work for Food (WFF) paradigm (*105*, *106*). WFF alters energy balance by providing a discrete number of calories for gradually increasing energy expenditure (Fig. 5H), without imposing any explicit feed:fast cycle (*105–108*). As energy balance approaches starvation-like conditions, mTORC1 activity and protein synthesis is greatly reduced

(*109–112*). Compared with control conditions (food *ad libitum*) where mice are nocturnal, as energy balance becomes negative under WFF, mice progressively become more diurnal (Fig. 5, I and J, fig. S14, B and C, (*105*)). As expected, this shift in locomotor activity is matched by a significant advance in the timing of core body temperature rhythms towards daylight hours (Fig. 5, K and L, fig. S14, D to F). This highlights the well-established relationship between locomotor rhythms and body temperature, and consistent with the proposed molecular mechanism of nocturnal-to-diurnal switching.

Discussion

Mammalian colonisation of the daytime niche accelerated when its previous occupants, the dinosaurs, became extinct (*1*). Subsequently, mammals came to occupy all temporal niches, and frequently switch between them as life history and environment dictates (*5*). The specific mechanism that permits this switch between nocturnality and diurnality was previously unknown, however. Here we investigated the mechanism of diurnal-nocturnal switching. We identified an apparent cell-intrinsic inversion of thermal signals to the cellular circadian clockwork. This arises from differences in the thermosensitivity of mTORC1-mediated changes in protein synthesis rate and basophilic kinase family activity, to oppositely affect the timing of circadian rhythms under daily temperature cycles, in cultured cells and tissues.

These critical differences in the cellular response to temperature mirror recent findings in developmental biology, where mammalian species show marked differences in global biochemical reaction rates (*56*, *57*, *78*). We made analogous discoveries around global phosphorylation and protein synthesis, before honing in on mTOR kinase as a most plausible candidate for contributing to the diurnal/nocturnal switch. We note that mTOR complexes 1 and 2 have several substrate effectors and are regulated by multiple different cell signalling systems (*113*). Therefore, we do not discount that differential temperature sensitivity of other cellular kinases, phosphatases, and signalling mechanisms, acting upstream, downstream or in parallel with mTOR, may also contribute to temporal niche switching. We note, moreover, that the re-organisation physiology under WFF requires several weeks and does not lead to fully diurnal behaviour. Therefore, we also do not discount roles for hypothalamic neuroplasticity or direct photic modulation of locomotor activity in temporal niche selection (*13*, *114–116*). Ultimately though, any switching mechanism that arose evolutionarily must have a genetic basis, and switching within an individual must occur epigenetically. In both cases, we have shown strong evidence that mTOR activity plays an important role. We consider genetic mechanisms of diurnality may be broadly dispersed and polygenic, where specifics may differ between diurnal lineages to achieve the same end. Future work might be directed towards identifying diurnal-nocturnal differences in temperature-dependence of mTOR pathway components and its regulators.

At the whole organism level, our findings results agree with the circadian thermo-energetics (CTE) hypothesis for conditional niche-switching in several different mammals (*4*). CTE states that, for homeothermic mammals, nocturnal activity patterns are more costly than diurnal patterns, since nocturnal animals have higher energy requirements that compensate for the greater heat loss of being active in the (cold) night (*104*, *117*, *118*). Diurnality arises as an energy saving measure when food availability is scarce, which outcompetes the extra predation pressure of being active by day (*119*). At the cellular level, these results support the bioenergetic hypothesis for circadian and other biological rhythms (*95*, *120*, *121*), where oscillations primarily function to minimise the high cost of maintaining protein homeostasis. The reduced temperature sensitivity of protein synthesis in diurnal mammals is thus an energy saving measure, buffering the energetically expensive process of translation against temperature, and minimising the cellular challenge of conflicting timing cues.

Overall our findings illustrate marked species differences in how temperature modulates protein synthesis rates to determine circadian phase, in cells, tissues and *in vivo*. Protein synthesis rates are more thermosensitive in nocturnal mammals than diurnal mammals, mirrored by clocks that speed up and slow down with temperature, respectively, with differential phase shifts after warming versus cooling. Global differences in kinase/phosphatase activity underly these translational differences, including differential thermosensitivity of mTORC1 activity. In mouse, SCN rhythms behave diurnally with respect to daily temperature rhythms and is resistant to perturbation; outside the SCN, the high thermosensitivity of mTORC1 and translational activity favours nocturnal behaviour and physiology under well-fed conditions. Buffering the temperature-dependence of such vital cell functions, which can arise through natural selection across generations or by environmental challenges that reduce basal mTOR/translational activity within a generation, attenuates the daily behaviour-driven thermal inputs to the cellular clockwork. When appraised over several days, this presents as a cell-intrinsic signal inverter. Resultant progressive phase differences between diurnal and nocturnal cellular clocks throughout the brain and body feedback to modulate, gradually and oppositely, behavioural and physiological timing across successive daily cycles. For nocturnal mammals in low energy balance or over evolutionary timescales for diurnal mammals, this manifests as a nocturnal-to-diurnal switch.

References and Notes

1. M. P. Gerkema, W. I. L. Davies, R. G. Foster, M. Menaker, R. A. Hut, The nocturnal bottleneck and the evolution of activity patterns in mammals. *Proc Royal Soc B Biological Sci*. 280, 20130508 (2013).

2. R. Refinetti, The diversity of temporal niches in mammals. *Biol Rhythm Res*. 39, 173–192 (2008).

3. R. Maor, T. Dayan, H. Ferguson-Gow, K. E. Jones, Temporal niche expansion in mammals from a nocturnal ancestor after dinosaur extinction. *Nat Ecol Evol*. 1, 1889–1895 (2017).

4. R. A. Hut, N. Kronfeld-Schor, V. van der Vinne, H. De la Iglesia, "Chapter 17. In search of a temporal niche: Environmental factors" in *Progress in Brain Research*, A. Kalsbeek, M. Merrow, T. Roenneberg, R. G. Foster, Eds. (Elsevier, 2012), vol. 199 of *Progress in Brain Research*, pp. 281–304.

5. D. R. van der Veen, S. J. Riede, P. D. Heideman, M. Hau, V. van der Vinne, R. A. Hut, Flexible clock systems: adjusting the temporal programme. *Philosophical Transactions Royal Soc B Biological Sci*. 372, 20160254 (2017).

6. M. dos Reis, J. Inoue, M. Hasegawa, R. J. Asher, P. C. J. Donoghue, Z. Yang, Phylogenomic datasets provide both precision and accuracy in estimating the timescale of placental mammal phylogeny. *Proc Royal Soc B Biological Sci*. 279, 3491–3500 (2012).

7. C. L. Partch, C. B. Green, J. S. Takahashi, Molecular architecture of the mammalian circadian clock. *Trends Cell Biol*. 24, 90–99 (2014).

8. D. C. Wong, J. S. O'Neill, Non-transcriptional processes in circadian rhythm generation. *Curr Opin Physiology*. 5, 117–132 (2018).

9. R. Chen, A. Schirmer, Y. Lee, H. Lee, V. Kumar, S.-H. Yoo, J. S. Takahashi, C. Lee, Rhythmic PER Abundance Defines a Critical Nodal Point for Negative Feedback within the Circadian Clock Mechanism. *Mol Cell*. 36, 417–430 (2009).

10. W. J. Schwartz, S. M. Reppert, S. M. Eagan, M. C. Moore-Ede, In vivo metabolic activity of the suprachiasmatic nuclei: a comparative study. *Brain Res*. 274, 184–187 (1983).

11. A. A. Nunez, A. Bult, T. L. McElhinny, L. Smale, Daily Rhythms of Fos Expression in Hypothalamic Targets of the Suprachiasmatic Nucleus in Diurnal and Nocturnal Rodents. *J Biol Rhythm*. 14, 300–306 (1999).

12. D. M. Berson, F. A. Dunn, M. Takao, Phototransduction by Retinal Ganglion Cells That Set the Circadian Clock. *Science*. 295, 1070–1073 (2002).

13. B. Bano-Otalora, M. J. Moye, T. Brown, R. J. Lucas, C. O. Diekman, M. D. Belle, Daily electrical activity in the master circadian clock of a diurnal mammal. *Elife*. 10, e68179 (2021).

14. A. P. Patton, M. H. Hastings, The suprachiasmatic nucleus. *Curr Biology Cb*. 28, R816–R822 (2018).

15. E. Challet, Minireview: Entrainment of the suprachiasmatic clockwork in diurnal and nocturnal mammals. *Endocrinology*. 148, 5648–55 (2007).

16. N. Inagaki, S. Honma, D. Ono, Y. Tanahashi, K. Honma, Separate oscillating cell groups in mouse suprachiasmatic nucleus couple photoperiodically to the onset and end of daily activity. *Proc National Acad Sci*. 104, 7664–7669 (2007).

17. R. Hut, E. V. der Zee, K. Jansen, M. Gerkema, S. Daan, Gradual reappearance of post-hibernation circadian rhythmicity correlates with numbers of vasopressin-containing neurons in the suprachiasmatic nuclei of European ground squirrels. *J Comp Physiol B*. 172, 59–70 (2002).

18. L. S. Mure, H. D. Le, G. Benegiamo, M. W. Chang, L. Rios, N. Jillani, M. Ngotho, T. Kariuki, O. Dkhissi-Benyahya, H. M. Cooper, S. Panda, Diurnal transcriptome atlas of a primate across major neural and peripheral tissues. *Science*. 359 (2018), doi:10.1126/science.aao0318.

19. R. Cohen, N. Kronfeld-Schor, C. Ramanathan, A. Baumgras, L. Smale, The Substructure of the Suprachiasmatic Nucleus: Similarities between Nocturnal and Diurnal Spiny Mice. *Brain Behav. Evol.* 75, 9–22 (2010).

20. C. Ramanathan, A. Stowie, L. Smale, A. A. Nunez, Phase preference for the display of activity is associated with the phase of extra-suprachiasmatic nucleus oscillators within and between species. *Neuroscience*. 170, 758–772 (2010).

21. C. M. Lambert, D. R. Weaver, Peripheral Gene Expression Rhythms in a Diurnal Rodent. *J Biol Rhythm*. 21, 77–79 (2006).

22. P. Kumar Jha, E. Challet, A. Kalsbeek, Circadian rhythms in glucose and lipid metabolism in nocturnal and diurnal mammals. *Mol Cell Endocrinol*. 418, 74–88 (2015).

23. G. D. M. Potter, D. J. Skene, J. Arendt, J. E. Cade, P. J. Grant, L. J. Hardie, Circadian Rhythm and Sleep Disruption: Causes, Metabolic Consequences, and Countermeasures. *Endocr Rev*. 37, 584–608 (2016).

24. C. Dibner, U. Schibler, Circadian timing of metabolism in animal models and humans. *J Intern Med*. 277, 513–527 (2015).

25. J. Bass, J. S. Takahashi, Circadian Integration of Metabolism and Energetics. *Science*. 330, 1349–1354 (2010).

26. C. Scheiermann, J. Gibbs, L. Ince, A. Loudon, Clocking in to immunity. *Nat Rev Immunol*. 18, 423–437 (2018).

27. M. D'Alessandro, S. Beesley, J. K. Kim, R. Chen, E. Abich, W. Cheng, P. Yi, J. S. Takahashi, C. Lee, A tunable artificial circadian clock in clock-defective mice. *Nat Commun*. 6, 8587 (2015).

28. K. A. Feeney, L. L. Hansen, M. Putker, C. Olivares-Yañez, J. Day, L. J. Eades, L. F. Larrondo, N. P. Hoyle, J. S. O'Neill, G. van Ooijen, Daily magnesium fluxes regulate cellular timekeeping and energy balance. *Nature*. 532, 375–379 (2016).

29. P. Crosby, R. Hamnett, M. Putker, N. P. Hoyle, M. Reed, C. J. Karam, E. S. Maywood, A. Stangherlin, J. E. Chesham, E. A. Hayter, L. Rosenbrier-Ribeiro, P. Newham, H. Clevers, D. A. Bechtold, J. S. O'Neill, Insulin/IGF-1 Drives PERIOD Synthesis to Entrain Circadian Rhythms with Feeding Time. *Cell*. 177, 896-909.e20 (2019).

30. R. M. Buijs, J. Wortel, J. J. V. Heerikhuize, M. G. P. Feenstra, G. J. T. Horst, H. J. Romijn, A. Kalsbeek, Anatomical and functional demonstration of a multisynaptic suprachiasmatic nucleus adrenal (cortex) pathway. *Eur J Neurosci*. 11, 1535–1544 (1999).

31. A. Balsalobre, S. A. Brown, L. Marcacci, F. Tronche, C. Kellendonk, H. M. Reichardt, G. Schütz, U. Schibler, Resetting of Circadian Time in Peripheral Tissues by Glucocorticoid Signaling. *Science*. 289, 2344–2347 (2000).

32. S. M. Ota, X. Kong, R. Hut, D. Suchecki, P. Meerlo, The impact of stress and stress hormones on endogenous clocks and circadian rhythms. *Frontiers Neuroendocrinol.* 63, 100931 (2021).

33. X. Kong, S. M. Ota, D. Suchecki, A. Lan, A. I. Peereboom, R. A. Hut, P. Meerlo, Chronic Social Defeat Stress Shifts Peripheral Circadian Clocks in Male Mice in a Tissue-Specific and Time-of-Day Dependent Fashion. *J. Biological Rhythm.* 37, 164–176 (2022).

34. X. Kong, M. Luxwolda, R. A. Hut, P. Meerlo, Adrenalectomy prevents the effects of social defeat stress on PER2 rhythms in some peripheral tissues in male mice. *Horm. Behav.* 150, 105326 (2023).

35. T. Roenneberg, S. Daan, M. Merrow, The Art of Entrainment. *J Biol Rhythm*. 18, 183–194 (2003).

36. C. H. Johnson, J. A. Elliott, R. Foster, Entrainment of Circadian Programs. *Chronobiol Int*. 20, 741–774 (2003).

37. F. Damiola, N. L. Minh, N. Preitner, B. Kornmann, F. Fleury-Olela, U. Schibler, Restricted feeding uncouples circadian oscillators in peripheral tissues from the

central pacemaker in the suprachiasmatic nucleus. *Gene Dev*. 14, 2950–2961 (2000).

38. K.-A. Stokkan, S. Yamazaki, H. Tei, Y. Sakaki, M. Menaker, Entrainment of the Circadian Clock in the Liver by Feeding. *Science*. 291, 490–493 (2001).

39. Y. Isojima, M. Nakajima, H. Ukai, H. Fujishima, R. G. Yamada, K. Masumoto, R. Kiuchi, M. Ishida, M. Ukai-Tadenuma, Y. Minami, R. Kito, K. Nakao, W. Kishimoto, S.-H. Yoo, K. Shimomura, T. Takao, A. Takano, T. Kojima, K. Nagai, Y. Sakaki, J. S. Takahashi, H. R. Ueda, CKIε/δ-dependent phosphorylation is a temperature-insensitive, period-determining process in the mammalian circadian clock. *Proc National Acad Sci*. 106, 15744–15749 (2009).

40. R. Refinetti, M. Menaker, The circadian rhythm of body temperature. *Physiol Behav*. 51, 613–637 (1992).

41. R. Refinetti, M. Menaker, The circadian rhythm of body temperature of normal and tau-mutant golden hamsters. *J Therm Biol*. 17, 129–133 (1992).

42. K. Krauchi, A. Wirz-Justice, Circadian rhythm of heat production, heart rate, and skin and core temperature under unmasking conditions in men. *Am J Physiology-regulatory Integr Comp Physiology*. 267, R819–R829 (1994).

43. S. A. Brown, G. Zumbrunn, F. Fleury-Olela, N. Preitner, U. Schibler, Rhythms of mammalian body temperature can sustain peripheral circadian clocks. *Curr Biol*. 12, 1574--1583 (2002).

44. L. M. Prolo, J. S. Takahashi, E. D. Herzog, Circadian Rhythm Generation and Entrainment in Astrocytes. *J Neurosci*. 25, 404–408 (2005).

45. E. D. Buhr, S.-H. Yoo, J. S. Takahashi, Temperature as a Universal Resetting Cue for Mammalian Circadian Oscillators. *Science*. 330, 379--385 (2010).

46. C. Saini, J. Morf, M. Stratmann, P. Gos, U. Schibler, Simulated body temperature rhythms reveal the phase-shifting behavior and plasticity of mammalian circadian oscillators. *Gene Dev*. 26, 567--580 (2012).

47. A. D. Beale, E. A. Hayter, P. Crosby, U. K. Valekunja, R. S. Edgar, J. E. Chesham, E. S. Maywood, F. H. Labeed, A. B. Reddy, K. P. Wright, K. S. Lilley, D. Bechtold, M. H. Hastings, J. S. O'Neill, Mechanisms and physiological function of daily haemoglobin oxidation rhythms in red blood cells. *bioRxiv* (2021), doi:10.1101/2021.10.11.463714.

48. J. Morf, G. Rey, K. Schneider, M. Stratmann, J. Fujita, F. Naef, U. Schibler, Cold-inducible RNA-binding protein modulates circadian gene expression posttranscriptionally. *Science*. 338, 379--383 (2012).

49. Y. Liu, W. Hu, Y. Murakawa, J. Yin, G. Wang, M. Landthaler, J. Yan, Cold-induced RNA-binding proteins regulate circadian gene expression by controlling alternative polyadenylation. *Sci Rep-uk*. 3, 1--11 (2013).

50. T. Haltenhof, A. Kotte, F. D. Bortoli, S. Schiefer, S. Meinke, A.-K. Emmerichs, K. K. Petermann, B. Timmermann, P. Imhof, A. Franz, B. Loll, M. C. Wahl, M. Preußner, F. Heyd, A Conserved Kinase-Based Body-Temperature Sensor Globally Controls Alternative Splicing and Gene Expression. *Mol Cell*. 78, 57-69.e4 (2020).

51. T. Miyake, Y. Inoue, X. Shao, T. Seta, Y. Aoki, K. T. N. Pham, Y. Shichino, J. Sasaki, T. Sasaki, M. Ikawa, Y. Yamaguchi, H. Okamura, S. Iwasaki, M. Doi, Minimal upstream open reading frame of Per2 mediates phase fitness of the circadian clock to day/night physiological body temperature rhythm. *Cell Reports*, 112157 (2023).

52. B. Kornmann, O. Schaad, H. Bujard, J. S. Takahashi, U. Schibler, System-driven and oscillator-dependent circadian transcription in mice with a conditionally active liver clock. *Plos Biol*. 5, 0179--0189 (2007).

53. H. Reinke, C. Saini, F. Fleury-Olela, C. Dibner, I. J. Benjamin, U. Schibler, Differential display of DNA-binding proteins reveals heat-shock factor 1 as a circadian transcription factor. *Gene Dev*. 22, 331--345 (2008).

54. I. Gotic, S. Omidi, F. Fleury-Olela, N. Molina, F. Naef, U. Schibler, Temperature regulates splicing efficiency of the cold-inducible RNA-binding protein gene Cirbp. *Gene Dev*. 30, 2005–2017 (2016).

55. M. Ebisuya, J. Briscoe, What does time mean in development? *Dev Camb Engl*. 145, dev164368 (2018).

56. M. Matsuda, H. Hayashi, J. Garcia-Ojalvo, K. Yoshioka-Kobayashi, R. Kageyama, Y. Yamanaka, M. Ikeya, J. Toguchida, C. Alev, M. Ebisuya, Species-specific segmentation clock periods are due to differential biochemical reaction speeds. *Science*. 369, 1450–1455 (2020).

57. T. Rayon, D. Stamataki, R. Perez-Carrasco, L. Garcia-Perez, C. Barrington, M. Melchionda, K. Exelby, J. Lazaro, V. L. J. Tybulewicz, E. M. C. Fisher, J. Briscoe, Species-specific pace of development is associated with differences in protein stability. *Science*. 369 (2020), doi:10.1126/science.aba7667.

58. J. S. O'Neill, A. B. Reddy, Circadian clocks in human red blood cells. *Nature*. 469, 498–503 (2011).

59. N. M. Rzechorzek, M. J. Thrippleton, F. M. Chappell, G. Mair, A. Ercole, M. Cabeleira, T. C.-T. H. R. I. (HR I. S.-S. P. and Investigators, J. Rhodes, I. Marshall, J. S. O'Neill, A daily temperature rhythm in the human brain predicts survival after brain injury. *Brain*. 145, 2031–2048 (2022).

60. K. E. Jones, J. Bielby, M. Cardillo, S. A. Fritz, J. O'Dell, C. D. L. Orme, K. Safi, W. Sechrest, E. H. Boakes, C. Carbone, C. Connolly, M. J. Cutts, J. K. Foster, R. Grenyer, M. Habib, C. A. Plaster, S. A. Price, E. A. Rigby, J. Rist, A. Teacher, O. R. P. Bininda-Emonds, J. L. Gittleman, G. M. Mace, A. Purvis, PanTHERIA: a species-level database of life history, ecology, and geography of extant and recently extinct mammals. *Ecology*. 90, 2648–2648 (2009).

61. V. E. Mendel, G. V. Raghavan, A study of diurnal temperature patterns in sheep. *J Physiology*. 174, 206–216 (1964).

62. D. M. Schumann, H. M. Cooper, M. D. Hofmeyr, N. C. Bennett, Circadian rhythm of locomotor activity in the four-striped field mouse, Rhabdomys pumilio: A diurnal African rodent. *Physiol. Behav.* 85, 231–239 (2005).

63. G. Donati, L. Santini, J. Razafindramanana, L. Boitani, S. Borgognini-Tarli, (Un-)expected nocturnal activity in "Diurnal" Lemur catta supports cathemerality as one of the key adaptations of the lemurid radiation. *Am J Phys Anthropol*. 150, 99–106 (2013).

64. L. Santini, D. Rojas, G. Donati, Evolving through day and night: origin and diversification of activity pattern in modern primates. *Behav Ecol*. 26, 789–796 (2015).

65. S.-H. Yoo, S. Yamazaki, P. L. Lowrey, K. Shimomura, C. H. Ko, E. D. Buhr, S. M. Siepka, H.-K. Hong, W. J. Oh, O. J. Yoo, M. Menaker, J. S. Takahashi, PERIOD2::LUCIFERASE real-time reporting of circadian dynamics reveals persistent circadian oscillations in mouse peripheral tissues. *P Natl Acad Sci Usa*. 101, 5339–5346 (2004).

66. J. Park, K. Lee, H. Kim, H. Shin, C. Lee, Endogenous circadian reporters reveal functional differences of PERIOD paralogs and the significance of PERIOD:CK1 stable interaction. *P Natl Acad Sci Usa*. 120, e2212255120 (2023).

67. K. A. Feeney, M. Putker, M. Brancaccio, J. S. O'Neill, In-depth Characterization of Firefly Luciferase as a Reporter of Circadian Gene Expression in Mammalian Cells. *J Biol Rhythm*. 31, 540–550 (2016).

68. G. Manella, D. Aizik, R. Aviram, M. Golik, G. Asher, Circa-SCOPE: high-throughput live single-cell imaging method for analysis of circadian clock resetting. *Nat Commun*. 12, 5903 (2021).

69. G. Manella, N. Bolshette, M. Golik, G. Asher, Input integration by the circadian clock exhibits nonadditivity and fold-change detection. *Proc National Acad Sci*. 119 (2022), doi:10.1073/pnas.2209933119.

70. M. Doi, H. Shimatani, Y. Atobe, I. Murai, H. Hayashi, Y. Takahashi, J.-M. Fustin, Y. Yamaguchi, H. Kiyonari, N. Koike, K. Yagita, C. Lee, M. Abe, K. Sakimura, H. Okamura, Non-coding cis-element of Period2 is essential for maintaining organismal

790 circadian behaviour and body temperature rhythmicity. *Nat Commun*. 10, 2563 (2019).

71. C.-H. Yu, Y. Dang, Z. Zhou, C. Wu, F. Zhao, M. S. Sachs, Y. Liu, Codon Usage Influences the Local Rate of Translation Elongation to Regulate Co-translational Protein Folding. *Mol Cell*. 59, 744–754 (2015).

795 72. V. Presnyak, N. Alhusaini, Y.-H. Chen, S. Martin, N. Morris, N. Kline, S. Olson, D. Weinberg, K. E. Baker, B. R. Graveley, J. Coller, Codon Optimality Is a Major Determinant of mRNA Stability. *Cell*. 160, 1111–1124 (2015).

73. Q. Wu, S. G. Medina, G. Kushawah, M. L. DeVore, L. A. Castellano, J. M. Hand, M. Wright, A. A. Bazzini, Translation affects mRNA stability in a codon-dependent
800 manner in human cells. *Elife*. 8, e45396 (2019).

74. Y. Liu, Q. Yang, F. Zhao, Synonymous but not Silent: The Codon Usage Code for Gene Expression and Protein Folding. *Annu Rev Biochem*. 90, 1–27 (2021).

75. M. Verma, J. Choi, K. A. Cottrell, Z. Lavagnino, E. N. Thomas, S. Pavlovic-Djuranovic, P. Szczesny, D. W. Piston, H. S. Zaher, J. D. Puglisi, S. Djuranovic, A
805 short translational ramp determines the efficiency of protein synthesis. *Nat Commun*. 10, 5774 (2019).

76. J. Fu, K. A. Murphy, M. Zhou, Y. H. Li, V. H. Lam, C. A. Tabuloc, J. C. Chiu, Y. Liu, Codon usage affects the structure and function of the Drosophila circadian clock protein PERIOD. *Gene Dev*. 30, 1761–1775 (2016).

810 77. M. Zhou, J. Guo, J. Cha, M. Chae, S. Chen, J. M. Barral, M. S. Sachs, Y. Liu, Non-optimal codon usage affects expression, structure and function of clock protein FRQ. *Nature*. 495, 111–115 (2013).

78. J. Lázaro, M. Costanzo, M. Sanaki-Matsumiya, C. Girardot, M. Hayashi, K. Hayashi, S. Diecke, T. B. Hildebrandt, G. Lazzari, J. Wu, S. Petkov, R. Behr, V.
815 Trivedi, M. Matsuda, M. Ebisuya, *Biorxiv*, in press, doi:10.1101/2022.10.13.512072.

79. C. S. Pittendrigh, On temperature independence in the clock system controlling emergence time in Drosophila. *Proc National Acad Sci*. 40, 1018–1029 (1954).

80. R. Narasimamurthy, D. M. Virshup, Molecular Mechanisms Regulating Temperature Compensation of the Circadian Clock. *Front Neurol*. 8, 1--5 (2017).

820 81. S. B. Khalsa, D. Whitmore, G. D. Block, Stopping the circadian pacemaker with inhibitors of protein synthesis. *Proc National Acad Sci*. 89, 10862–10866 (1992).

82. S. Yamaguchi, H. Isejima, T. Matsuo, R. Okura, K. Yagita, M. Kobayashi, H. Okamura, Synchronization of Cellular Clocks in the Suprachiasmatic Nucleus. *Science*. 302, 1408–1412 (2003).

825 83. A. Schröder-Lorenz, L. Rensing, Circadian changes in protein-synthesis rate and protein phosphorylation in cell-free extracts of Gonyaulax polyedra. *Planta*. 170, 7–13 (1987).

84. C. G. Proud, Phosphorylation and Signal Transduction Pathways in Translational Control. *Csh Perspect Biol*. 11, a033050 (2019).

830 85. H. L. Rust, P. R. Thompson, Kinase Consensus Sequences: A Breeding Ground for Crosstalk. *Acs Chem Biol*. 6, 881–892 (2011).

86. J. L. Johnson, T. M. Yaron, E. M. Huntsman, A. Kerelsky, J. Song, A. Regev, T.-Y. Lin, K. Liberatore, D. M. Cizin, B. M. Cohen, N. Vasan, Y. Ma, K. Krismer, J. T. Robles, B. van de Kooij, A. E. van Vlimmeren, N. Andrée-Busch, N. F. Käufer, M. V.
835 Dorovkov, A. G. Ryazanov, Y. Takagi, E. R. Kastenhuber, M. D. Goncalves, B. D. Hopkins, O. Elemento, D. J. Taatjes, A. Maucuer, A. Yamashita, A. Degterev, M. Uduman, J. Lu, S. D. Landry, B. Zhang, I. Cossentino, R. Linding, J. Blenis, P. V. Hornbeck, B. E. Turk, M. B. Yaffe, L. C. Cantley, An atlas of substrate specificities for the human serine/threonine kinome. *Nature*, 1–8 (2023).

840 87. K. Ninomiya, N. Kataoka, M. Hagiwara, Stress-responsive maturation of Clk1/4 pre-mRNAs promotes phosphorylation of SR splicing factor. *J Cell Biol*. 195, 27–40 (2011).

88. X. Liu, P. C. C. Liu, N. Santoro, D. J. Thiele, Conservation of a stress response: human heat shock transcription factors functionally substitute for yeast HSF. *The*
845 *EMBO J.* 16, 6466–6477 (1997).

89. M. E. LLeonart, A new generation of proto-oncogenes: Cold-inducible RNA binding proteins. *Biochimica et Biophys. Acta BBA - Rev. Cancer*. 1805, 43–52 (2010).

90. M. B. Al-Fageeh, C. M. Smales, Control and regulation of the cellular responses
850 to cold shock: the responses in yeast and mammalian systems. *Biochem. J.* 397, 247–259 (2006).

91. C. C. Dibble, B. D. Manning, Signal integration by mTORC1 coordinates nutrient input with biosynthetic output. *Nat Cell Biol*. 15, 555–564 (2013).

92. R. Zoncu, A. Efeyan, D. M. Sabatini, mTOR: from growth signal integration to
855 cancer, diabetes and ageing. *Nat Rev Mol Cell Bio*. 12, 21–35 (2011).

93. C. C. Thoreen, L. Chantranupong, H. R. Keys, T. Wang, N. S. Gray, D. M. Sabatini, A unifying model for mTORC1-mediated regulation of mRNA translation. *Nature*. 485, 109–113 (2012).

94. A. Stangherlin, J. L. Watson, D. C. S. Wong, S. Barbiero, A. Zeng, E.
860 Seinkmane, S. P. Chew, A. D. Beale, E. A. Hayter, A. Guna, A. J. Inglis, M. Putker, E. Bartolami, S. Matile, N. Lequeux, T. Pons, J. Day, G. van Ooijen, R. M. Voorhees,

D. A. Bechtold, E. Derivery, R. S. Edgar, P. Newham, J. S. O'Neill, Compensatory ion transport buffers daily protein rhythms to regulate osmotic balance and cellular physiology. *Nat Commun*. 12, 6035 (2021).

95. A. Stangherlin, E. Seinkmane, J. S. O'Neill, Understanding circadian regulation of mammalian cell function, protein homeostasis, and metabolism. *Curr Opin Syst Biology*. 28, 100391 (2021).

96. C. Jouffe, G. Cretenet, L. Symul, E. Martin, F. Atger, F. Naef, F. Gachon, The Circadian Clock Coordinates Ribosome Biogenesis. *Plos Biol*. 11 (2013), doi:10.1371/journal.pbio.1001455.

97. C. Dolde, J. Bischof, S. Gruter, A. Montada, J. Halekotte, C. Peifer, H. Kalbacher, U. Baumann, U. Knippschild, B. Suter, A CK1 FRET biosensor reveals that DDX3X is an essential activator of CK1ϵ. *J Cell Sci*. 131 (2018), doi:10.1242/jcs.207316.

98. M. Abe, E. D. Herzog, S. Yamazaki, M. Straume, H. Tei, Y. Sakaki, M. Menaker, G. D. Block, Circadian Rhythms in Isolated Brain Regions. *J Neurosci*. 22, 350–356 (2002).

99. U. Abraham, A. E. Granada, P. O. Westermark, M. Heine, A. Kramer, H. Herzel, Coupling governs entrainment range of circadian clocks. *Mol Syst Biol*. 6, 438 (2010).

100. N. F. Ruby, D. E. Burns, H. C. Heller, Circadian Rhythms in the Suprachiasmatic Nucleus are Temperature-Compensated and Phase-Shifted by Heat Pulses In Vitro. *J Neurosci*. 19, 8630–8636 (1999).

101. V. Pilorz, P. S. Cunningham, A. Jackson, A. C. West, T. T. Wager, A. S. I. Loudon, D. A. Bechtold, A novel mechanism controlling resetting speed of the circadian clock to environmental stimuli. *Curr Biology Cb*. 24, 766–73 (2013).

102. S. Nishide, D. Ono, Y. Yamada, S. Honma, K. Honma, De novo synthesis of PERIOD initiates circadian oscillation in cultured mouse suprachiasmatic nucleus after prolonged inhibition of protein synthesis by cycloheximide. *Eur J Neurosci*. 35, 291–299 (2012).

103. S. Daan, K. Spoelstra, U. Albrecht, I. Schmutz, M. Daan, B. Daan, F. Rienks, I. Poletaeva, G. Dell'Omo, A. Vyssotski, H.-P. Lipp, Lab Mice in the Field: Unorthodox Daily Activity and Effects of a Dysfunctional Circadian Clock Allele. *J Biol Rhythm*. 26, 118–129 (2011).

104. V. van der Vinne, S. J. Riede, J. A. Gorter, W. G. Eijer, M. T. Sellix, M. Menaker, S. Daan, V. Pilorz, R. A. Hut, Cold and hunger induce diurnality in a nocturnal mammal. *Proc National Acad Sci*. 111, 15256–15260 (2014).

105. R. A. Hut, V. Pilorz, A. S. Boerema, A. M. Strijkstra, S. Daan, Working for Food Shifts Nocturnal Mouse Activity into the Day. *Plos One*. 6, e17527 (2011).

106. G. Perrigo, Breeding and feeding strategies in deer mice and house mice when females are challenged to work for their food. *Anim Behav*. 35, 1298–1316 (1987).

107. L. van Rosmalen, S. J. Riede, V. Pilorz, T. Adage, A. J. W. Scheurink, V. van der Vinne, R. A. Hut, "Nocturnal and Diurnal Behavior Assessed by the "Work-for-Food" Protocol in Small Rodents" in *Circadian Clocks* (2022), *Neuromethods*, pp. 187–216.

108. V. Acosta-Rodríguez, F. Rijo-Ferreira, M. Izumo, P. Xu, M. Wight-Carter, C. B. Green, J. S. Takahashi, Circadian alignment of early onset caloric restriction promotes longevity in male C57BL/6J mice. *Sci New York N Y*. 376, 1192–1202 (2022).

109. M. A. McNurlan, A. M. Tomkins, P. J. Garlick, The effect of starvation on the rate of protein synthesis in rat liver and small intestine. *Biochem J*. 178, 373–9 (1979).

110. F. Yoshizawa, T. Nagasawa, N. Nishizawa, R. Funabiki, Protein Synthesis and Degradation Change Rapidly in Response to Food Intake in Muscle of Food-Deprived Mice ,. *J Nutrition*. 127, 1156–1159 (1997).

111. T. Naito, A. Kuma, N. Mizushima, Differential Contribution of Insulin and Amino Acids to the mTORC1-Autophagy Pathway in the Liver and Muscle*. *J. Biological Chem.* 288, 21074–21081 (2013).

112. A. Kulkarni, A. Dong, V. V. Kulkarni, J. Chen, O. Laxton, A. Anand, S. Maday, Differential regulation of autophagy during metabolic stress in astrocytes and neurons. *Autophagy*. 16, 1651–1667 (2020).

113. S. Battaglioni, D. Benjamin, M. Wälchli, T. Maier, M. N. Hall, mTOR substrate phosphorylation in growth control. *Cell*. 185, 1814–1836 (2022).

114. S. E. Doyle, T. Yoshikawa, H. Hillson, M. Menaker, Retinal pathways influence temporal niche. *Proc. National Acad. Sci.* 105, 13133–13138 (2008).

115. R. A. Schoonderwoerd, P. T. Gutiérrez, R. Blommers, A. W. Beurden, T. C. J. J. Coenen, N. J. Klett, S. H. Michel, J. H. Meijer, Inhibitory responses to retinohypothalamic tract stimulation in the circadian clock of the diurnal rodent Rhabdomys pumilio. *The FASEB J.* 36, e22415 (2022).

116. R. A. Schoonderwoerd, R. Caputo, A. Ramkisoensing, J. A. M. Janse, H. C. van Diepen, S. Raison, N. A. V. Derks, D. Sage-Ciocca, T. Deboer, E. Challet, J. H. Meijer, *Biorxiv*, in press, doi:10.1101/2022.05.31.493966.

117. V. van der Vinne, J. A. Gorter, S. J. Riede, R. A. Hut, Diurnality as an energy-saving strategy: energetic consequences of temporal niche switching in small mammals. *J. Exp. Biology*. 218, 2585–2593 (2015).

118. S. J. Riede, V. van der Vinne, R. A. Hut, The flexible clock: predictive and reactive homeostasis, energy balance and the circadian regulation of sleep–wake timing. *J Exp Biol*. 220, 738–749 (2017).

119. V. van der Vinne, P. Tachinardi, S. J. Riede, J. Akkerman, J. Scheepe, S. Daan, R. A. Hut, Maximising survival by shifting the daily timing of activity. *Ecol Lett*. 22, 2097–2102 (2019).

120. E. Seinkmane, S. Y. Peak-Chew, A. Zeng, N. M. Rzechorzek, A. D. Beale, D. C. Wong, J. S. O'Neill, *Biorxiv*, in press, doi:10.1101/2022.09.30.509905.

121. D. C. S. Wong, E. Seinkmane, A. Zeng, A. Stangherlin, N. M. Rzechorzek, A. D. Beale, J. Day, M. Reed, S. Y. Peak-Chew, C. T. Styles, R. S. Edgar, M. Putker, J. S. O'Neill, CRYPTOCHROMES promote daily protein homeostasis. *Embo J*, e2021108883 (2021).

122. C. S. Pittendrigh, Circadian Rhythms and the Circadian Organization of Living Systems. *Cold Spring Harb Sym*. 25, 159--184 (1960).

123. A. Seluanov, A. Vaidya, V. Gorbunova, Establishing Primary Adult Fibroblast Cultures From Rodents. *J Vis Exp* (2010), doi:10.3791/2033.

124. J. Drouin-Ouellet, S. Lau, P. L. Brattås, D. R. Ottosson, K. Pircs, D. A. Grassi, L. M. Collins, R. Vuono, A. A. Sjöland, G. Westergren-Thorsson, C. Graff, L. Minthon, H. Toresson, R. A. Barker, J. Jakobsson, M. Parmar, REST suppression mediates neural conversion of adult human fibroblasts via microRNA-dependent and -independent pathways. *EMBO Mol. Medicine*. 9, 1117–1131 (2017).

125. U. K. Valekunja, R. S. Edgar, M. Oklejewicz, G. T. J. van der Horst, J. S. O'Neill, F. Tamanini, D. J. Turner, A. B. Reddy, Histone methyltransferase MLL3 contributes to genome-scale circadian transcription. *Proc National Acad Sci*. 110, 1554–1559 (2013).

126. K. Labun, T. G. Montague, J. A. Gagnon, S. B. Thyme, E. Valen, CHOPCHOP v2: a web tool for the next generation of CRISPR genome engineering. *Nucleic Acids Res*. 44, W272--W276 (2016).

127. A. Zeng, J. S. O'Neill, "Using ALLIGATORs to Capture Circadian Bioluminescence" in *Circadian Regulation* (2022), vol. 2482 of *Methods in Molecular Biology*, pp. 125–135.

128. P. Crosby, N. P. Hoyle, J. S. O'Neill, Flexible Measurement of Bioluminescent Reporters Using an Automated Longitudinal Luciferase Imaging Gas- and

Temperature-optimized Recorder (ALLIGATOR). *J Vis Exp* (2017), doi:10.3791/56623.

129. P. Stothard, The Sequence Manipulation Suite: JavaScript Programs for Analyzing and Formatting Protein and DNA Sequences. *BioTechniques*. 28, 1102–1104 (2000).

130. Y. Nakamura, T. Gojobori, T. Ikemura, Codon usage tabulated from international DNA sequence databases: status for the year 2000. *Nucleic Acids Res.* 28, 292–292 (2000).

131. A. R. Gruber, R. Lorenz, S. H. Bernhart, R. Neuböck, I. L. Hofacker, The Vienna RNA websuite. *Nucleic Acids Res*. 36, W70-4 (2008).

132. H. L. Sladitschek, P. A. Neveu, MXS-Chaining: A Highly Efficient Cloning Platform for Imaging and Flow Cytometry Approaches in Mammalian Systems. *Plos One*. 10, e0124958 (2015).

133. N. Bouquier, E. Moutin, L. A. Tintignac, A. Reverbel, E. Jublanc, M. Sinnreich, Y. Chastagnier, J. Averous, P. Fafournoux, C. Verpelli, T. Boeckers, G. Carnac, J. Perroy, V. Ollendorff, AIMTOR, a BRET biosensor for live imaging, reveals subcellular mTOR signaling and dysfunctions. *Bmc Biol*. 18, 81 (2020).

134. J. Jumper, R. Evans, A. Pritzel, T. Green, M. Figurnov, O. Ronneberger, K. Tunyasuvunakool, R. Bates, A. Žídek, A. Potapenko, A. Bridgland, C. Meyer, S. A. A. Kohl, A. J. Ballard, A. Cowie, B. Romera-Paredes, S. Nikolov, R. Jain, J. Adler, T. Back, S. Petersen, D. Reiman, E. Clancy, M. Zielinski, M. Steinegger, M. Pacholska, T. Berghammer, S. Bodenstein, D. Silver, O. Vinyals, A. W. Senior, K. Kavukcuoglu, P. Kohli, D. Hassabis, Highly accurate protein structure prediction with AlphaFold. *Nature*. 596, 583–589 (2021).

135. M. Varadi, S. Anyango, M. Deshpande, S. Nair, C. Natassia, G. Yordanova, D. Yuan, O. Stroe, G. Wood, A. Laydon, A. Žídek, T. Green, K. Tunyasuvunakool, S. Petersen, J. Jumper, E. Clancy, R. Green, A. Vora, M. Lutfi, M. Figurnov, A. Cowie, N. Hobbs, P. Kohli, G. Kleywegt, E. Birney, D. Hassabis, S. Velankar, AlphaFold Protein Structure Database: massively expanding the structural coverage of protein-sequence space with high-accuracy models. *Nucleic Acids Res*. 50, D439–D444 (2021).

136. R. Cencic, J. Pelletier, Hippuristanol - A potent steroid inhibitor of eukaryotic initiation factor 4A. *Translation*. 4, e1137381 (2016).

137. S. Yamazaki, R. Numano, M. Abe, A. Hida, R. Takahashi, M. Ueda, G. D. Block, Y. Sakaki, M. Menaker, H. Tei, Resetting Central and Peripheral Circadian Oscillators in Transgenic Rats. *Science*. 288, 682–685 (2000).

138. T. Yoshikawa, S. Yamazaki, M. Menaker, Effects of Preparation Time on Phase of Cultured Tissues Reveal Complexity of Circadian Organization. *J Biol Rhythm*. 20, 500–512 (2005).

139. T. Noguchi, M. Ikeda, Y. Ohmiya, Y. Nakajima, A Dual-Color Luciferase Assay System Reveals Circadian Resetting of Cultured Fibroblasts by Co-Cultured Adrenal Glands. *Plos One*. 7, e37093 (2012).

140. M. H. Hastings, A. B. Reddy, D. G. McMahon, E. S. Maywood, Analysis of Circadian Mechanisms in the Suprachiasmatic Nucleus by Transgenesis and Biolistic Transfection. *Methods Enzymol*. 393, 579–592 (2005).

141. O. Wagih, N. Sugiyama, Y. Ishihama, P. Beltrao, Uncovering Phosphorylation-Based Specificities through Functional Interaction Networks*. *Mol Cell Proteomics*. 15, 236–245 (2016).

142. J. Ou, H. Liu, N. K. Nirala, A. Stukalov, U. Acharya, M. R. Green, L. J. Zhu, dagLogo: An R/Bioconductor package for identifying and visualizing differential amino acid group usage in proteomics data. *Plos One*. 15, e0242030 (2020).

143. J. Ponten, E. Saksela, Two established in vitro cell lines from human mesenchymal tumours. *Int J Cancer*. 2, 434–447 (1967).

144. K. A. Lamia, U. M. Sachdeva, L. DiTacchio, E. C. Williams, J. G. Alvarez, D. F. Egan, D. S. Vasquez, H. Juguilon, S. Panda, R. J. Shaw, C. B. Thompson, R. M. Evans, AMPK Regulates the Circadian Clock by Cryptochrome Phosphorylation and Degradation. *Science*. 326, 437–440 (2009).

145. C. H. Gabriel, M. del Olmo, A. Zehtabian, M. Jäger, S. Reischl, H. van Dijk, C. Ulbricht, A. Rakhymzhan, T. Korte, B. Koller, A. Grudziecki, B. Maier, A. Herrmann, R. Niesner, T. Zemojtel, H. Ewers, A. E. Granada, H. Herzel, A. Kramer, Live-cell imaging of circadian clock protein dynamics in CRISPR-generated knock-in cells. *Nat Commun*. 12, 3796 (2021).

146. M. Zhou, T. Wang, J. Fu, G. Xiao, Y. Liu, Nonoptimal codon usage influences protein structure in intrinsically disordered regions. *Mol Microbiol*. 97, 974–87 (2015).

147. J. F. Pelham, J. C. Dunlap, J. M. Hurley, Intrinsic disorder is an essential characteristic of components in the conserved circadian circuit. *Cell Commun Signal*. 18, 181 (2020).

148. Y. Liu, A code within the genetic code: codon usage regulates co-translational protein folding. *Cell Commun Signal*. 18, 145 (2020).

149. K. M. Sakamoto, K. B. Kim, A. Kumagai, F. Mercurio, C. M. Crews, R. J. Deshaies, Protacs: Chimeric molecules that target proteins to the Skp1–Cullin–F box complex for ubiquitination and degradation. *Proc. National Acad. Sci.* 98, 8554–8559 (2001).

150. M. Békés, D. R. Langley, C. M. Crews, PROTAC targeted protein degraders: the past is prologue. *Nat. Rev. Drug Discov.* 21, 181–200 (2022).

151. J. Aschoff, Exogenous and Endogenous Components in Circadian Rhythms. *Cold Spring Harb Sym*. 25, 11–28 (1960).

Acknowledgements: We thank Rachel Edgar and Ken Wright for intellectual contributions in the genesis of the project; Rajesh Narasimamurthy and David Virshup for pilot experiments; Michael Hastings, Robert Lucas and Roger Barker for resources and discussion; Beat Suter and Joachim Bischof for providing CK1 sensor domain; Tim Eppley for valuable discussions on activity patterns in Lemurs; Joana Frankel for general discussion on diurnal models; Kevin Moreau for advice on PROTACs. We thank all past and current members of O'Neill lab and David Bechtold, for their valuable feedback. We thank biomedical services group staff at Medical Research Council (MRC) Ares facility and LMB facilities for assistance.

For the purpose of open access, the MRC Laboratory of Molecular Biology applies a CC BY public copyright licence to any Author Accepted Manuscript version arising.

Funding:
NMR was supported by the Medical Research Council (MR/S022023/1).
JON was supported by the Medical Research Council (MC_UP_1201/4).
RR was supported by a Wellcome Trust Investigator Award (210684/Z/18/Z) to Robert Lucas, University of Manchester.

Author contributions:
Conceptualization: ADB, JSO, NMR
Formal Analysis: ADB, NMR, SYP-C, VP, RAH
Funding acquisition: NMR, JSO
Investigation: ADB, NMR, AZ, AM, NJS, VP, NRJ, SYP-C, RAH
Methodology: ADB, JSO
Project administration: ADB, JSO
Resources: NJS, RR, MAL, MFB, SVF, ZV, JP
Software: ADB
Supervision: JSO
Visualization: ADB, NMR
Writing – original draft: ADB
Writing – review & editing: ADB, JSO, NMR, AM, RAH, MAL, NJS, PC

Competing interests: The authors declare that they have no competing interests.

Data and materials availability: All data are available in the main text and supplementary material. Code are available at https://github.com/andrewbeale. Materials are available upon request to JSO, and are subject to materials transfer agreements.

Supplementary Materials

Materials and Methods

Figs. S1 to S14

Table S1

References (*129-151*)

1095 **Fig. 1. Entrainment to temperature is a cellular correlate of behavioural temporal niche**

(A) With respect to the external day-night cycle, organismal and cellular physiology differ between nocturnal mice and diurnal humans, despite these species having the same cell-autonomous circadian clock mechanism. The retinorecipient hypothalamic
1100 SCN functions very similarly in diurnal and nocturnal mammals, with neuronal firing and PER oscillations peaking in the daytime, allowing the SCN to serve as an internal representation of the day-night cycle. However, outside of the SCN, organismal behaviour, physiology and cellular activity, including oscillations of PER, are oppositely organised between diurnal and nocturnal mammals and instead vary
1105 with daily systemic signals that consistently coincide with the transition from rest/fast to activity/feeding rather than external solar time. This suggests a switch, downstream of the SCN, that controls the appearance of diurnality.

(B) After entrainment in repeated 37 °C (red) and 32 °C (blue) 12h:12h cycles which emulate the daily body temperature rhythm, mouse and human primary fibroblasts
1110 (N = 3 and 5 biological replicates respectively) are set to opposing phases when released into constant 37 °C (red). Bioluminescence from *Bmal1:luc* was recorded under cycling and constant temperature portions of the experiment. A dotted line illustrates the inverse phases under constant conditions.

(C) Primary fibroblasts from striped mouse (*Rhabdomys pumilio*), marmoset
1115 (*Callithrix jacchus*), gibbon (*Hylobates lar*), sheep (*Ovis aries*), rat (*Rattus norvegicus*) and lemur (*Lemur catta*) were cultured under 37 °C and 32 °C 12h:12h for 7 cycles before release into constant 37 °C. Bioluminescence from *Bmal1:luc* was recorded in constant conditions immediately after the last 32 °C to 37 °C transition at t = 0h. A dotted line at t= 32h illustrates the different phases under
1120 constant conditions.

(D) Circadian phase of the *Bmal1:luc* rhythm in constant conditions for the 7 species from (B) and (C). Circadian phase (0h – 24h) is given as the time of the peak of *Bmal1:luc* expression relative to the subjective 37 °C:32 °C cycle, where phase 0h is equal to the start of the 37 °C period and phase 12h is equal to the start of the 32°C
1125 period. Two distinct clusters of opposing circadian phases of entrainment are found in mammalian cells which do not exclusively group with body size.

(E) Human (U2OS) and mouse (fibroblasts, immortalised) expressing PER2-LUC from its endogenous locus, entrain to cycles of temperature (12 h 37 °C: 12 h 32 °C) with opposing phases. Note the high amplitude rhythms during temperature cycles
1130 that damp upon entry into constant temperature condition, and the different phase of entrainment between the two different reporters, Bmal1:luc (A) and PER2-LUC (D).

(F) Human (U2OS) and mouse (fibroblasts, immortalised) PER2-LUC cells were synchronised by medium change at t=-186h and subject to temperature cycles (12 h 37 °C: 12 h 35.5 °C) set 6h out of alignment to original phase. Human and mouse
1135 cells re-entrain to the new timing cue within 7 days, and exhibit a stable and opposite entrained phase in constant conditions.

(G) Circadian phase, given as peak of PER2-LUC expression relative to the last transition from 32°C to 37°C, calculated from (D) and (E). Subjective hot and cold portions of the cycle are given by white shading from 0 – 12h and blue shading from
1140 12-24h. Statistics: Two-way ANOVA (TWA) followed by Šídák's post-hoc test.

Fig. 2. Differential response to temperature is both a specific property of PER2 and global translation

1145 **(A)** Raw data showing preceding 24h and ensuing 36h of cells exposed to a temperature shift up at 0 h (trough of PER2). Change in baseline, Δ baseline, due to temperature dependence of $^{app}K_m$ of luciferase, and integration of luciferase signal, ∫ synthesis, due to synthesis of new PER2-LUC, are indicated by shading.

(B) and **(C)** Quantification of Δ baseline, (B), and ∫ synthesis, (C), after a temperature 1150 shift up at 0 h in mouse and human lines. Mean ± SEM and individual points presented throughout. Statistics: Student's t-test, unpaired.

(D) U2OS cells stably expressing constitutive PER2-LUC fusions – human PER2-LUC (orange), mouse PER2-LUC (grey) or codon-optimised human PER2-LUC (teal) – were kept for 3 days at constant temperature of either 32 °C or 37 °C before 1155 shifting temperature at t = 0 min. Fold induction of luminescence is shown relative to t = 0 min.

(E) Rate of induction was quantified as the gradient of the straight line fit from non-linear regression (Prism), given as fold/hour. Induction rates were compared between reporters. Statistics: TWA followed by Šídák's post-hoc test.

1160 **(F)** U2OS cells expressing HaloTag from the endogenous PER2 locus were treated with 1 μM HaloPROTAC3 or DMSO control for 24h before lysis and immunoblotting. Anti-Halotag antibody was used to detect the presence of the fusion PER2-HALO protein, anti β-actin serves as a loading control.

(G) PER2-HaloTag U2OS cells were cultured under temperature cycles ± 1 μM 1165 HaloPROTAC3 (n=4 each condition). At 0h cells were kept in constant temperature. Bioluminescence from Bmal1:luc was recorded throughout. Difference in phase of entrainment between control and PROTAC treatment is given, mean ± SEM. PROTAC treatment elicits an advance in entrained phase to temperature relative to control.

1170 **(H)** Human cells (U2OS) or mouse cells (NIH 3t3) stably expressing constitutive LUC as a reporter of protein synthesis were exposed to the same temperature conditions as (D).

(I) Rate of induction of constitutive LUC calculated as (E).

(J) Schematic of the temperature step experiment including puromycin incorporation. 1175 Human and mouse fibroblasts were kept for 1 week in constant temperature of either 32°C (blue) or 37°C (red) and at 0 h cells were either stepped up (blue:red), down (red:blue) or kept at the constant temperature as a control (either 32 °C, blue:blue, or 37 °C, red:red). At 1.5 h, 10 μg/ml puromycin was added to the cells which were lysed 30 min later. Fold change puromycin incorporation was calculated by 1180 comparing incorporation in the stepped condition vs incorporation in the control condition.

(K) Representative immunoblot of one of three biological replicates of mouse or human cells exposed to the four conditions (red:red constant 37 °C, red:blue step from 37 °C to 32 °C, blue:blue constant 32 °C, blue:red step from 32 °C to 37 °C). 1185 Anti-puromycin (top) and coomassie loading control (bottom).

(L) Fold change puromycin incorporation, $^{\text{incorporation in shifted}}$ / $_{\text{incorporation in constant control}}$, in three biological replicates. Statistics: TWA mixed-effects model, matched design, followed by Šídák's post-hoc test. Interaction species x temperature $F(1, 4) = 24.99$, $p = 0.0075$.

1190 **(M)** Protein synthesis rate (from Fig. 2K and fig. S7A) at constant 32°C (blue) or 37 °C (red) in (left) paired biological replicate fibroblast cells of mouse (N=3) or human (N=3), or (right) rat (n=3) or striped mouse (n=3) fibroblasts. Statistics: (left) TWA mixed-effects model, matched design. Interaction species x temperature $F(1, 4) = 7.986$, $p = 0.0475$, Šídák's post-hoc test reported; (right) TWA. Interaction species x
1195 temperature $F(1, 8) = 31.38$, $p = 0.0005$, Šídák's post-hoc test reported.
(N) Free-running period at constant 32°C (blue) or 37 °C (red) in (left) paired biological replicate fibroblast cells of mouse (N=3) or human (N=3) expressing Bmal1:luc, or (right) rat (n=3) or striped mouse (n=3) fibroblasts expressing Bmal1:luc. Statistics: (left) TWA mixed-effects model, matched design. Interaction
1200 species x temperature, $F(1, 4) = 23.68$, $p = 0.0082$, Šídák's post-hoc test reported; (right) TWA. Interaction species x temperature $F(1, 20) = 170.8$, $p < 0.0001$, Šídák's post-hoc test reported.
(O) Q_{10} of circadian period, calculated from free-running period at the two temperatures in (N). Note that whilst Q_{10} is approximately 1 in all species, a defining
1205 feature of circadian rhythms (*122*), nocturnal mammals and diurnal mammals are under- and over-compensated respectively. Statistics: OWA, Šídák's post-hoc test reported vs mouse.

1210

Fig. 3. Differential temperature-dependent mTOR activation underlies differential protein synthesis rhythms
(A) Schematic of temperature step experiment for (phospho)proteomics. Human and mouse primary fibroblasts were kept for 1 week in constant temperature of either
1215 32°C (blue) or 37°C (red). At t = -24h, cells were treated with 100nM dexamethasone to synchronise and t = 0 h cells either stepped up (blue:red), down (red:blue) or kept at the constant temperature as a control (either 32 °C, blue:blue, or 37 °C, red:red). Cells were lysed 1h later and quantitative proteomics (TMT-MS/MS) was performed to analyse the (phospho)proteome. For each phosphosite or peptide, fold change
1220 upon a temperature step is calculated by dividing (phospho)peptide signal of the stepped condition by the constant condition from which they were stepped. Long-term adaptation to temperature was examined by calculation of fold change (phospho)peptide signal from constant 37 °C by signal at constant 32 °C.
(B) Phosphoproteomics matrices for mouse (6904 phosphopeptides) and human
1225 (5690 phosphopeptides). Matrix shows fold changes upon step up (x-axis) and step down (y-axis) for each phosphopeptide. Phosphopeptides are classified where fold change significantly increases with increasing temperature (proportional, ∝ temp, teal) or significantly decreases with increasing temperature (inversely proportional, ∝ 1/temp, purple). Phosphopeptides that do not change significantly, or change
1230 significantly but in a single direction, are shown in grey.
(C) Motif analysis was performed on phosphopeptides that changed proportionally (∝ temp) or inversely proportionally (∝ 1/temp). Sequence logos showing over-represented AA residues with significant differential AA usage (DAU) are shown for phosphopeptides that change proportionally (above) and inverse proportionally
1235 (below) for mouse (top) and human (bottom). Sequence logos are centred around the phosphoacceptor at position 0. Sequence logos showing under-represented AA residues (i.e. depleted) are shown in fig. S10.

(D) Probability density distribution of fold change upon temperature step (top) or adaptation (below) for every detected phosphopeptide. Mouse (grey) and human (orange). Statistics: Mann-Whitney, p-value shown.
(E) Schematic of split luciferase biosensors. A phosphopeptide recognition domain, forkhead-associated domain (FHA), is bound to an N-terminal fragment of firefly luciferase (1-416). A sensor domain consisting of 5-21 amino acids from a kinase target, including the annotated target S/T, is bound to a C-terminal fragment of firefly luciferase (396-550). Upon phosphorylation of the sensor domain's target S/T, the two fragments conjugate, leading to luminescence.
(F and G) Split luciferase sensors of CK1 activity (F) and mTORC1 activity (G) were stably expressed in mouse (NIH 3t3) or human (U2OS) cells (n=4 each) which were subjected to 12 h 37 °C: 12 h 32 °C temperature cycles. Cells were placed in temperature cycles at 0h and normalised bioluminescence on days 2, 3 and 4 of the cycling condition are shown. Under temperature cycles, CK1 activity peaks in the cold portion of the cycle in both species, whereas mTORC1 activity is in antiphase.
(H) Human and mouse cells expressing constitutive LUC (SV40:LUC), a proxy for protein synthesis, were cultured in temperature cycles as (F) and (G). Protein synthesis oscillates in antiphase in the two species, similar to mTORC1 activity.

Fig. 4. Manipulation of global translation rate alters phase of entrainment
(A) Global protein synthesis, PER2 synthesis, protein phosphorylation, and mTORC1 activity, here depicted as poles of a circle, respond to temperature change in a species-specific manner. Over multiple cycles of identical temperature changes, this resets the cellular clock to different phases in nocturnal and diurnal mammals.
(B) Human and mouse PER2-LUC fibroblasts, cultured in decreasing concentrations of serum, were entrained to 7 days of temperature cycles before transfer to constant conditions. Dashed line at the peak of 10% serum control is shown for illustration purposes.
(C) Change in phase, relative to 10% serum control, is shown. Statistics: Two-way ANOVA followed by Šídák's post-hoc test, n=6 (human) or 19-24 (mouse).
(D) Human and mouse PER2-LUC fibroblasts were entrained in temperature cycles in the presence of mTORC1/2 inhibitor (1 μM INK128) or control, then left to free-run at 37C. Dashed line at the peak of DMSO control is shown for illustration purposes.
(E) Striped mouse and rat fibroblasts expressing Bmal1:luc were entrained in temperature cycles in the presence of mTORC1/2 inhibitor (1 μM INK128) or control, then left to free-run at 37C. Dashed line at the peak of 10% serum control is drawn for illustration purposes.
(F) Change in phase, relative to control, is shown for mTORC1/2 inhibitor. Statistics: $Phase_{control}$ vs $phase_{treatment}$ two-way ANOVA followed by Šídák's post-hoc test, n=4-6 each condition.
(G) Human and mouse PER2-LUC cells, kept in constant conditions, were treated with inhibitors of the cap-binding complex that target eIF4A (rocaglamide, rocA; hippuristanol) at the trough of PER2-LUC at t=-12h, indicated by an arrow. Dashed line at the peak of DMSO control is shown for illustration purposes.
(H) Change in phase, relative to control, in mouse and human after treatment. Statistics: Two-way ANOVA followed by Šídák's post-hoc test, n=4 each condition.

Fig. 5. Global translation rate underlies phase of entrainment in tissues and the nocturnal-diurnal switch

(A) Experiment schematic. Tissues (pituitary, pit; adrenal gland, ad; lung; suprachiasmatic nuclei, SCN) were dissected from PER2-LUC mice and exposed to either temperature cycles coincident with or antiphasic to their previous activity patterns, or constant temperature. INK128 or control was added at the start of culture and luminescence from PER2-LUC was measured to compare circadian phase of entrainment.

(B) PER2-LUC mouse pituitary, adrenal or lung tissues were dissected from mice at the beginning of lights on (i.e. the start of the rest phase for nocturnal mice) at time = 0h. Tissue slices were cultured *ex vivo* in the presence of luciferin, treated with DMSO (left) or INK128 (right), and exposed to cycles of temperature (12 h 37 °C: 12 h 32 °C) antiphasic to previous activity patterns. Days 2 and 3 of temperature cycles and 3 days of constant conditions are shown.

(C) Circadian phase of entrainment calculated from (B), given relative to the final transition from 32 °C to 37°C. Statistics: TWA mixed-effects model, matched design. Interaction tissue x drug $F(2, 24) = 4.28$, $p = 0.025$; Šídák's post-hoc test reported, n=5 each condition.

(D) SCN tissue was dissected from PER2-LUC mice, sliced, and placed into *ex vivo* culture in the presence of luciferin. Slices were entrained for 7 days in antiphasic temperature cycles (12 h: 12 h 37 °C: 32 °C, black line, or 32 °C: 37 °C, grey line) before release into constant 37 °C.

(E) Circadian phase of entrainment calculated from (D), relative to time = 0h. Statistics: Student's t-test, unpaired, n=4-5.

(F) SCN slices from PER2-LUC mice kept under LD cycles (subjective LD cycle shown) were exposed for 3 days to temperature cycles (12 h: 12 h 37 °C: 32 °C) in antiphase to the LD cycle from which the mice were taken, or kept at constant temperature (37 °C). *Ex vivo* culture started at 0h when slices were given either INK128 (blue) or DMSO (black/grey), and bioluminescence was monitored throughout. PER2-LUC expression is plotted against circadian time, where 0h = the start of the subjective light period.

(G) Circadian phase of entrainment with respect to LD cycle calculated from (F). Statistics: TWA. Interaction cycle x drug $F(1, 13) = 1.36$, $p = 0.26$; Šídák's post-hoc test, n=3-5 each condition.

(H) Experimental schematic for the Work for Food (WFF) paradigm as conducted by Hut et al. (*105*). Adult male mice were singly housed in cages equipped water *ad libitum* and running wheels under 12h : 12h light:dark cycles. The number of food pellets given was controlled by the number of revolutions each mouse made on the running wheel. In the *ad libitum* baseline portion of the experiment, one pellet was given per ~100 revolutions. The number of revolutions per pellet was gradually increased in the WFF group until one pellet was given per ~300 revolutions. Running wheel activity and core body temperature from implanted temperature logger was recorded throughout.

(I) Average proportion of total daily locomotor activity in 1h bins across the 24h day. Activity in N=10-12 mice was averaged over 7 days of recording during the test period of the experiment (days 40-47). Mice were kept in 6am ON: 6pm OFF LD cycle throughout, and grey shading indicates dark phase.

(J) Diurnality index for *ad lib* control (n=10) and WFF (n=11) groups over the test period (days 40-47). Diurnality index during baseline (days 2-10) and test (days 40-47) was compared in control and WFF groups by TWA mixed-effects model, matched design. Interaction, baseline vs test x ad lib vs WFF $F(1, 19) = 53.57$, $p < 0.0001$, Šídák's post-hoc test reported for test period.

(K) Average daily body temperature in 1h bins across the 24h day. Core body temperature in N=10-12 mice was averaged over 7 days of recording during days 40-47.

(L) The acrophase of body temperature for *ad lib* control (n=8) and WFF (n=11) over the test period (days 40-47). Acrophase during baseline (days 2-10) and test (days 40-47) was compared in control and WFF groups by TWA mixed-effects model, matched design. Interaction, baseline vs test x ad lib vs WFF $F(1, 17) = 123.5$, $p < 0.0001$, Šídák's post-hoc test reported for test period.

1350

Figure 1

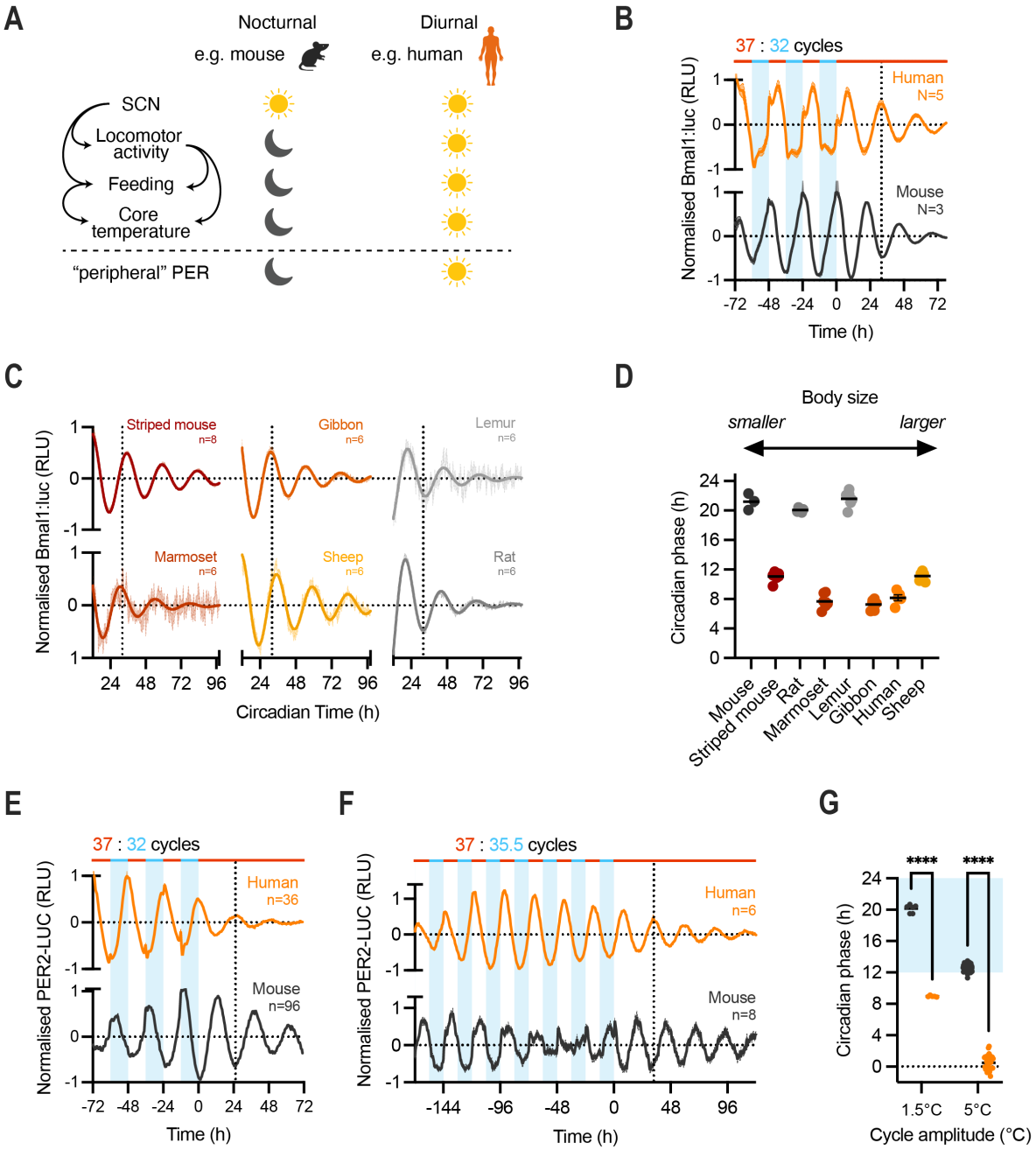

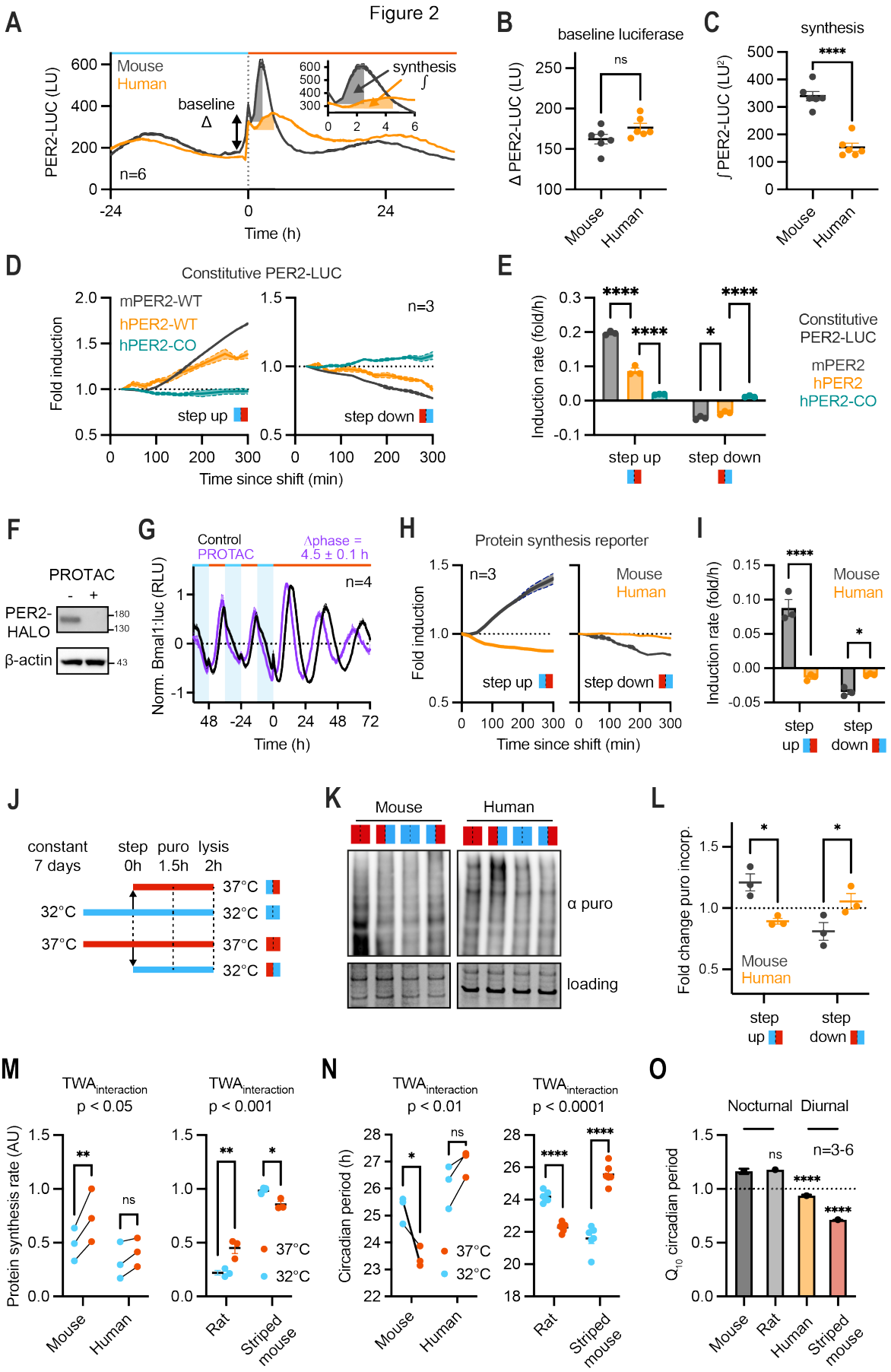
Figure 2
A
Mouse
Human
baseline
Δ
synthesis
∫
PER2-LUC (LU)
n=6
Time (h)
B
baseline luciferase
ns
Δ PER2-LUC (LU)
Mouse
Human
C
synthesis
****
∫ PER2-LUC (LU²)
D
Constitutive PER2-LUC
mPER2-WT
hPER2-WT
hPER2-CO
n=3
Fold induction
step up
step down
Time since shift (min)
E
Induction rate (fold/h)
Constitutive PER2-LUC
mPER2
hPER2
hPER2-CO
F
PROTAC
PER2-HALO
β-actin
G
Control
PROTAC
Δphase = 4.5 ± 0.1 h
n=4
Norm. Bmal1:luc (RLU)
Time (h)
H
Protein synthesis reporter
n=3
Mouse
Human
Fold induction
Time since shift (min)
I
Induction rate (fold/h)
J
constant 7 days
step 0h
puro 1.5h
lysis 2h
37°C
32°C
K
Mouse
Human
α puro
loading
L
Fold change puro incorp.
M
TWA interaction p < 0.05
TWA interaction p < 0.001
Protein synthesis rate (AU)
Rat
Striped mouse
N
TWA interaction p < 0.01
TWA interaction p < 0.0001
Circadian period (h)
O
Nocturnal
Diurnal
n=3-6
Q10 circadian period

Figure 3

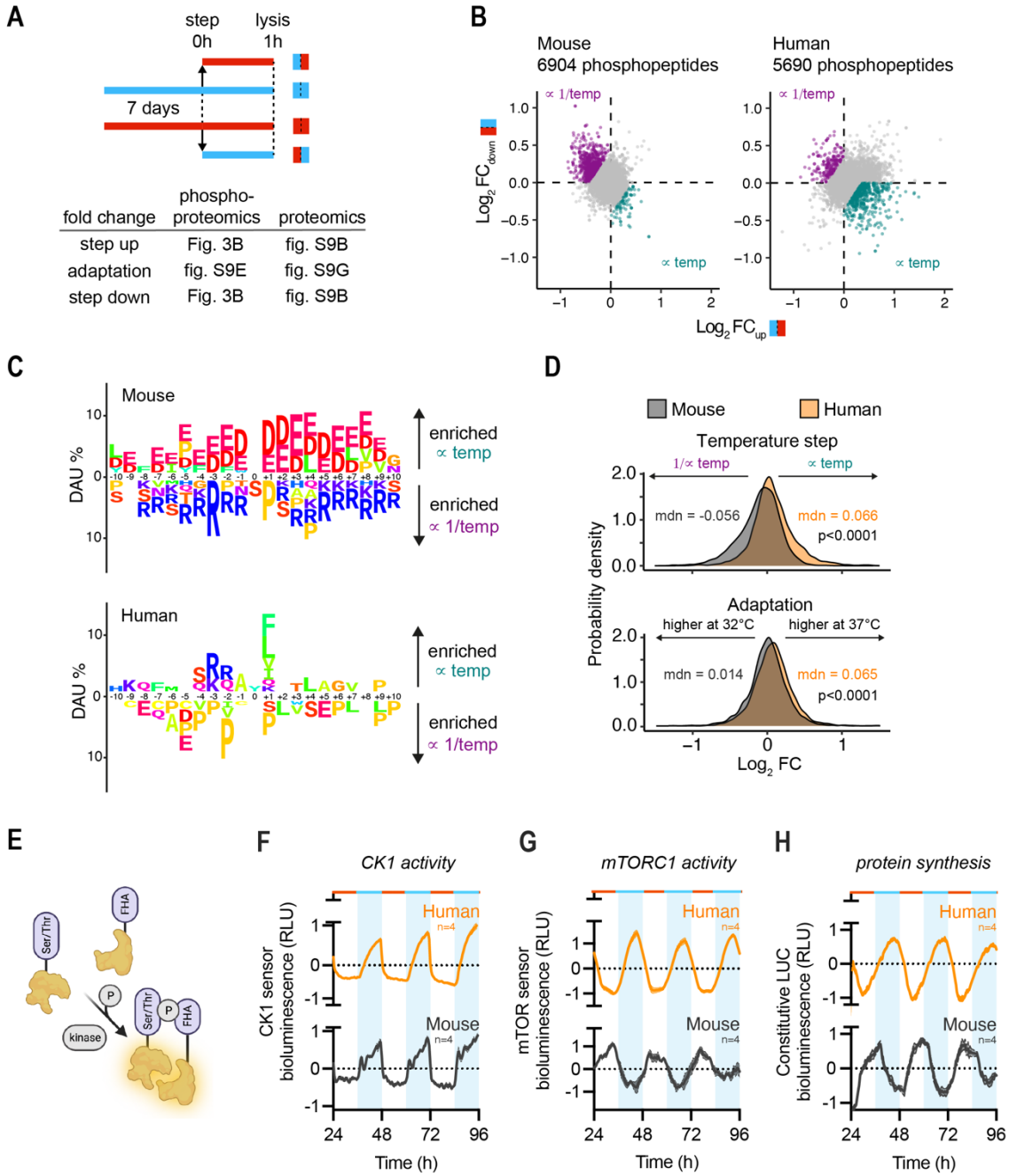

fold change	phospho-proteomics	proteomics
step up	Fig. 3B	fig. S9B
adaptation	fig. S9E	fig. S9G
step down	Fig. 3B	fig. S9B

1355

Figure 4

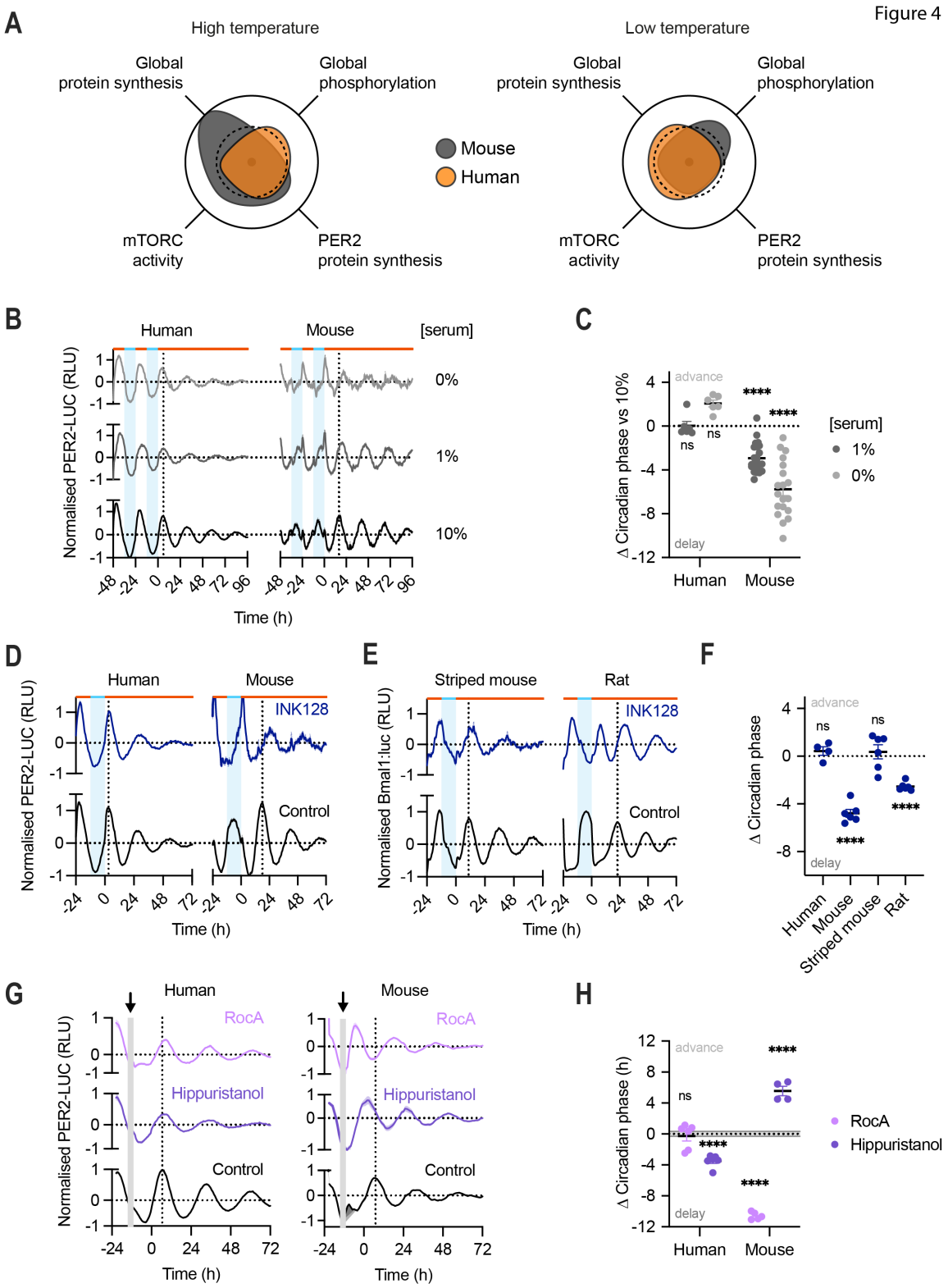
A
High temperature
Low temperature
Global protein synthesis
Global phosphorylation
mTORC activity
PER2 protein synthesis
Mouse
Human
B
Human
Mouse
[serum]
0%
1%
10%
Normalised PER2-LUC (RLU)
Time (h)
C
advance
delay
ns
****
Δ Circadian phase vs 10%
[serum]
1%
0%
Human
Mouse
D
Human
Mouse
INK128
Control
Normalised PER2-LUC (RLU)
Time (h)
E
Striped mouse
Rat
INK128
Control
Normalised Bmal1:luc (RLU)
Time (h)
F
advance
delay
ns
****
Δ Circadian phase
Human
Mouse
Striped mouse
Rat
G
Human
Mouse
RocA
Hippuristanol
Control
Normalised PER2-LUC (RLU)
Time (h)
H
advance
delay
ns
****
Δ Circadian phase (h)
RocA
Hippuristanol
Human
Mouse

Figure 5

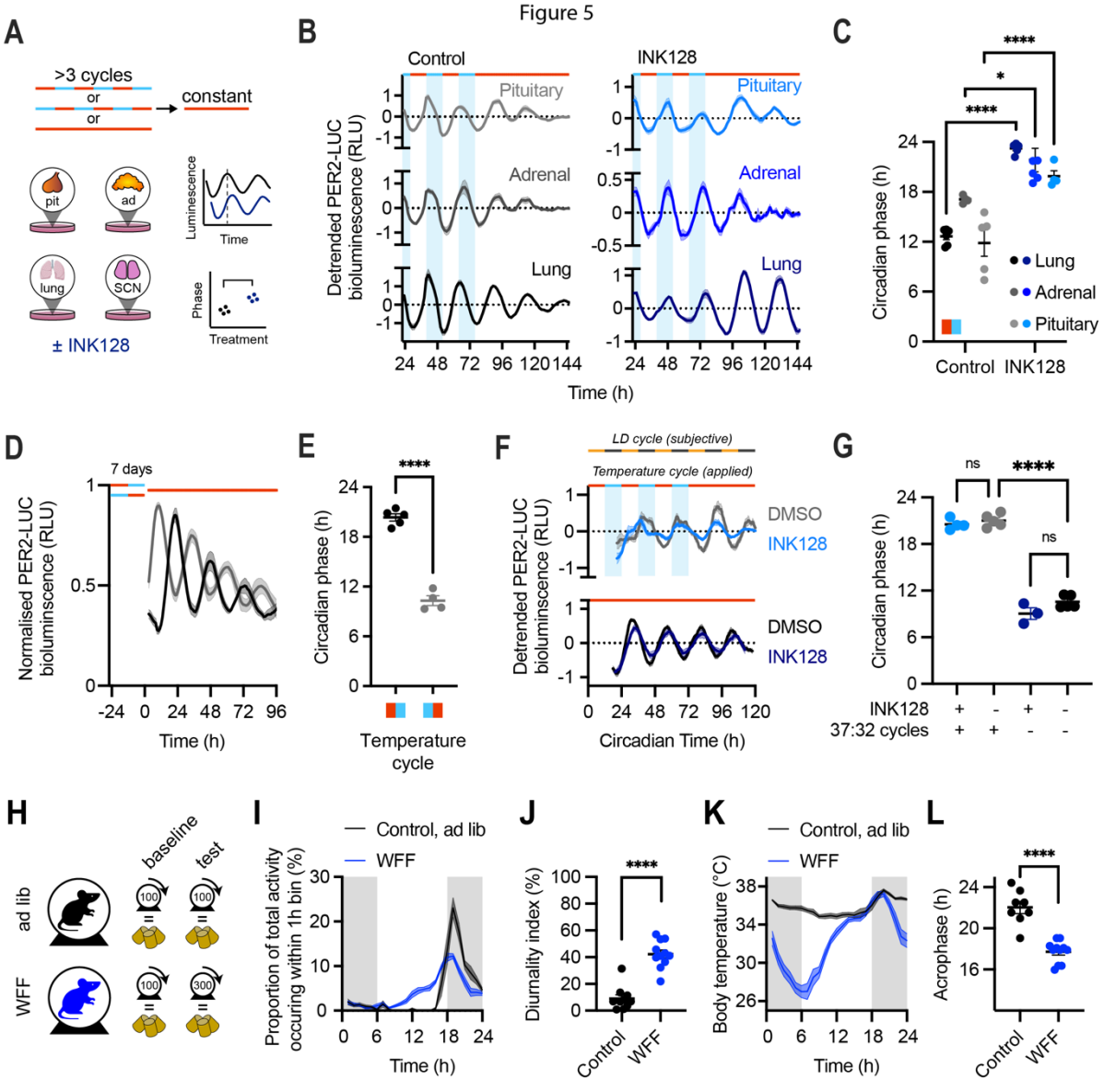
A
>3 cycles
or
or
constant
pit
ad
lung
SCN
± INK128
Luminescence
Time
Phase
Treatment
B
Control
INK128
Pituitary
Adrenal
Lung
Detrended PER2-LUC bioluminescence (RLU)
Time (h)
C
Circadian phase (h)
Lung
Adrenal
Pituitary
Control
INK128
D
7 days
Normalised PER2-LUC bioluminscence (RLU)
Time (h)
E
Circadian phase (h)
Temperature cycle
F
LD cycle (subjective)
Temperature cycle (applied)
DMSO
INK128
Detrended PER2-LUC bioluminscence (RLU)
Circadian Time (h)
G
ns
Circadian phase (h)
INK128
37:32 cycles
H
baseline
test
ad lib
WFF
I
Control, ad lib
WFF
Proportion of total activity occuring within 1h bin (%)
Time (h)
J
Diurnality index (%)
Control
WFF
K
Control, ad lib
WFF
Body temperature (°C)
Time (h)
L
Acrophase (h)
Control
WFF